

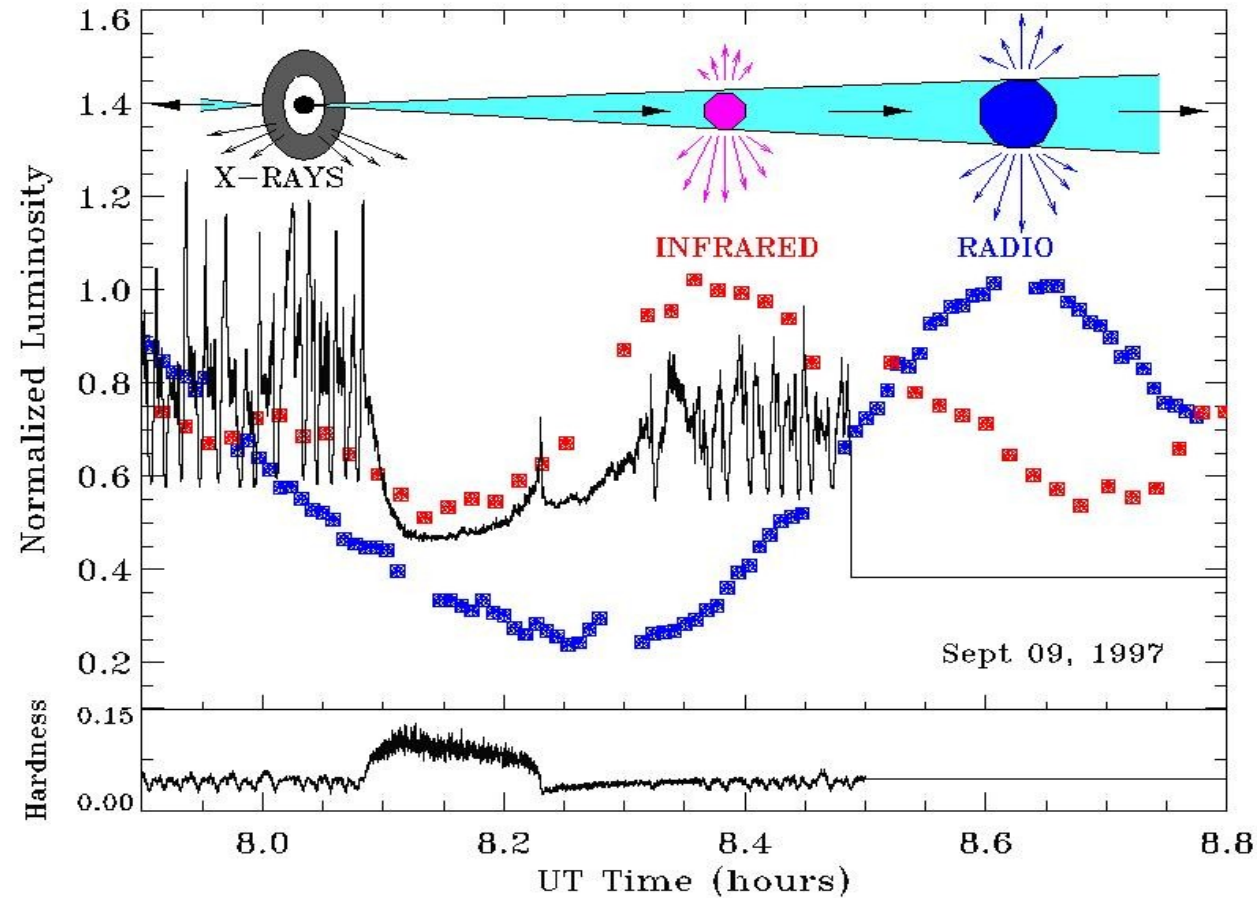
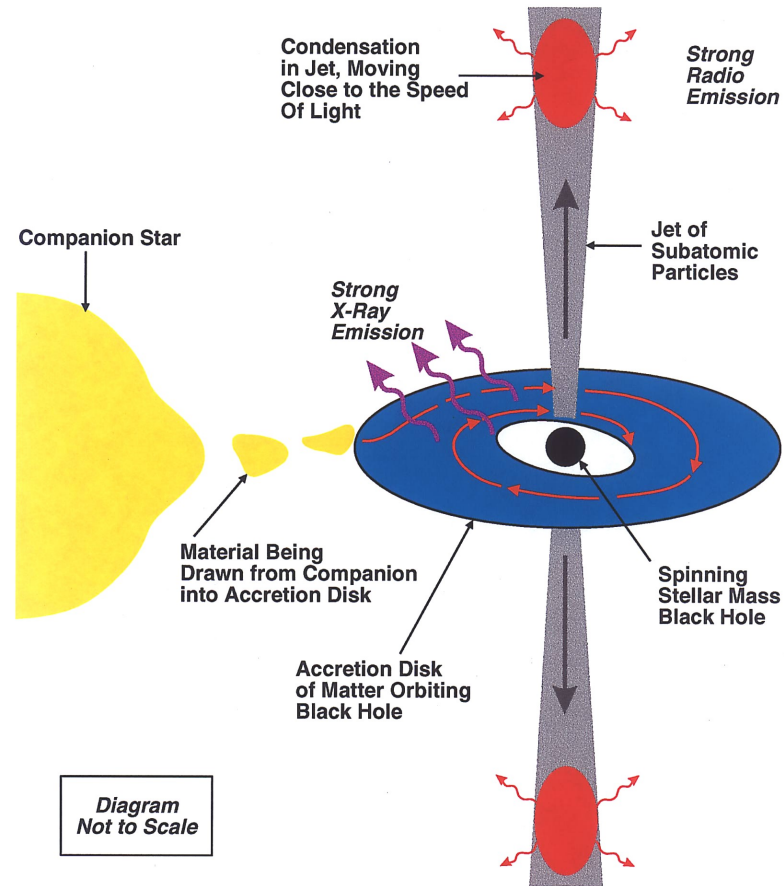
Radio Observations

ACCRETION-JET CONNECTION

$$\Delta\tau \propto M_{\text{BH}}$$

1 hr in GRS 1915+105 = 30 yr in SgrA*

Mirabel et al. 1998



• THE TRIGGERS OF JETS ARE INSTABILITIES IN THE ACCRETION DISK (TRANSITION LOW HARD TO HIGH THE X-RAY “SPIKE” MARKS THE ONSET OF A SHOCK THROUGH THE COMPACT, STEADY JET

• ANALOGOUS ACCRETION-JET CONNECTION IN 3C 120 Marscher (2002)

Table 1. XRB systems with resolved radio jets.

Name	Companion	Accretor	Jet size (AU)
HMXBs			
LS I +61 303	B0V	NS/BH?	10–700
V 4641 Sgr	B9III	Black Hole	–
LS 5039	O6.5V((f))	NS/BH?	10–1000
SS 433	evolved A	NS/BH?	$10^4 - 10^6$
Cygnus X-1	O9.7Iab	Black Hole	40
Cygnus X-3	WNe	NS/BH?	10^4
LMXBs			
Circinus X-1	Subgiant	Neutron Star	10^4
XTE J1550-564	G8-K5V	Black Hole	10^3
Scorpius X-1	Subgiant	Neutron Star	40
GRO J1655-40	F3/5IV	Black Hole	8000
GRS 1915+105	K-M III	Black Hole	$10 - 10^4$
GX 339-4		Black Hole	<4000
1E 1740.7-2942		NS/BH?	10^6
XTE J1748-288		NS/BH?	10^4
GRS 1758-258		NS/BH?	10^6

Massi (2005); Paredes (2005); Casares (2005).

Y

VLA 27 Km

VLBA



Mauna Kea
Hawaii

Owens Valley
California

Brewster
Washington

North Liberty
Iowa

Hancock
New Hampshire

Kit Peak
Arizona

Pie Town
New Mexico

Fort Davis
Texas

Los Alamos
New Mexico

St. Croix
Virgin Islands

MERLIN
Multi Element Radio Linked Interferometer Network

Tabley
Darnhall
Wardle
Knockin
Defford
Cambridge

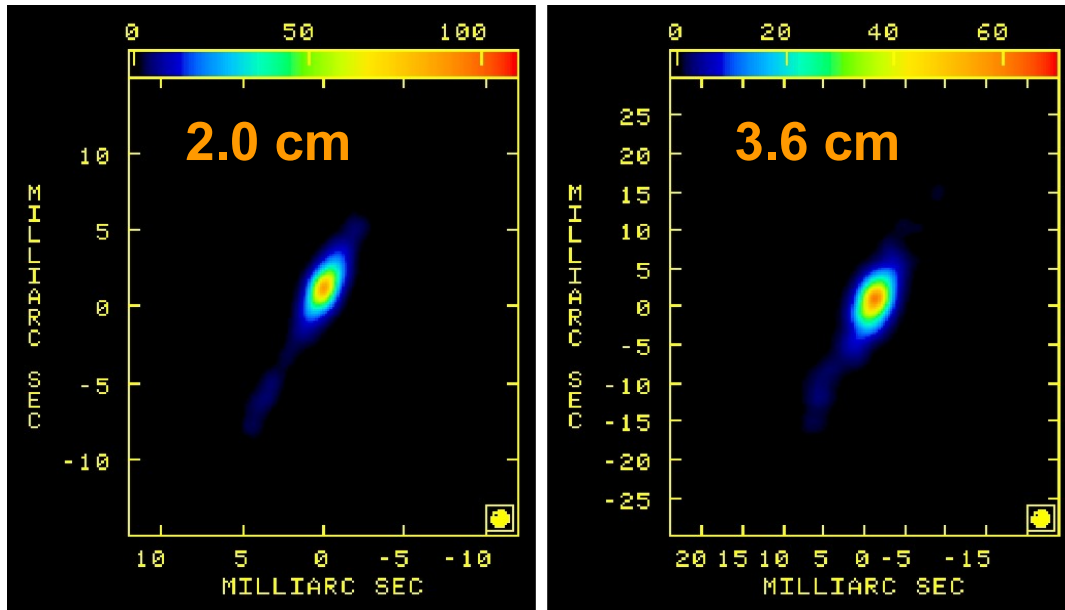
Jodrell Bank

MERLIN 150 Km



COMPACT STEADY JETS

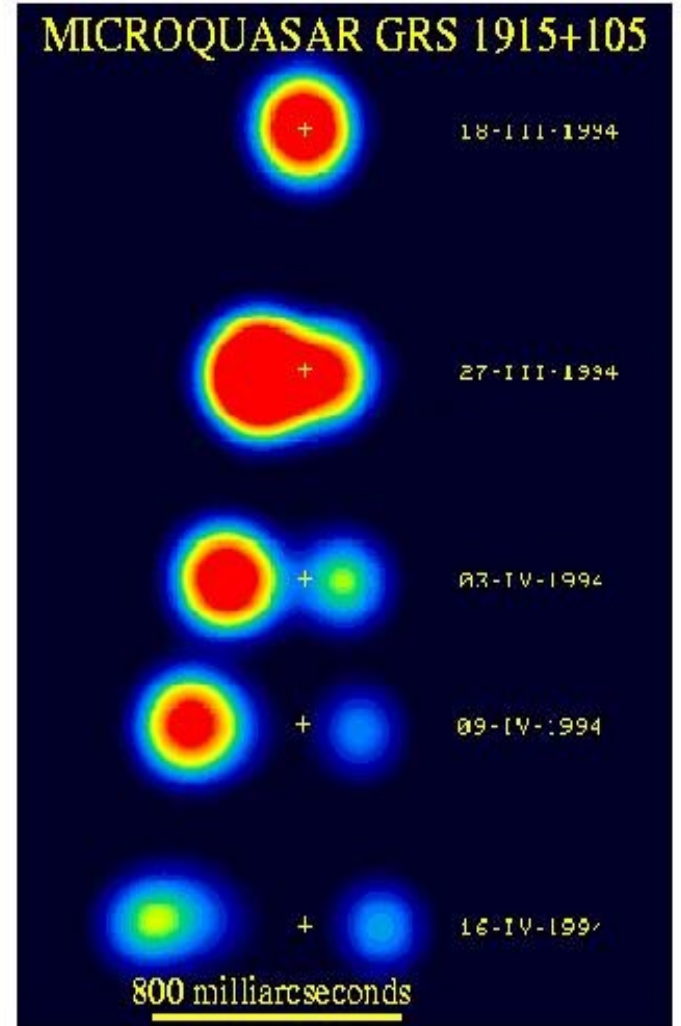
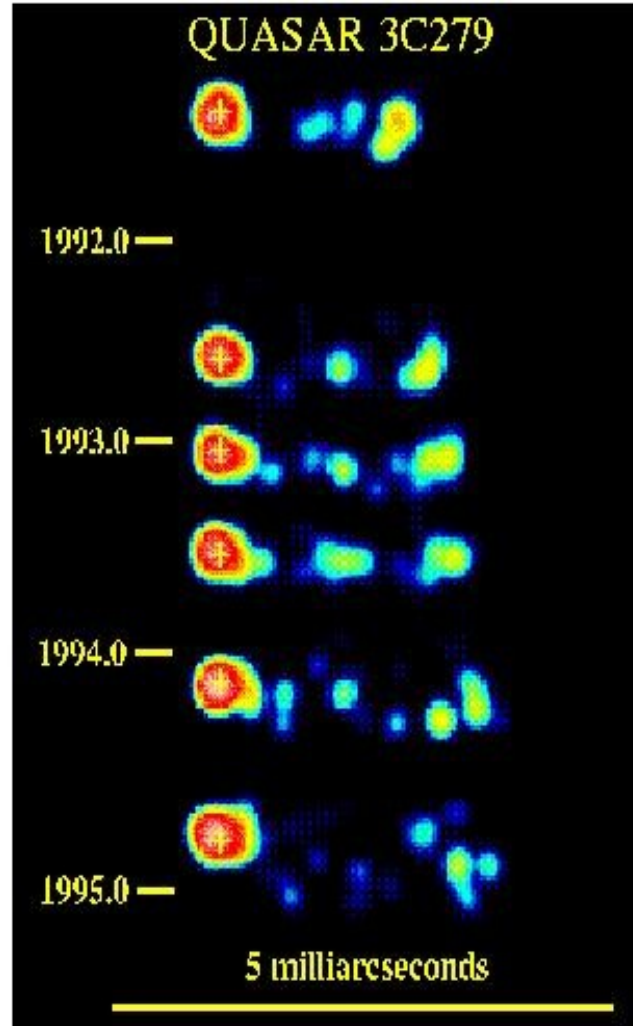
GRS 1915+105: Dhawan, Ribo & Mirabel (2006)



- ~100 AU IN LENGTH PRESENT DURING LOW HARD STATE
- SPEED OF THE FLOW $< 0.4c$ (Dhawan, Ribo & Mirabel 2006)

SUPERLUMINAL MOTION IN THE GALAXY

Mirabel & Rodriguez, 1994



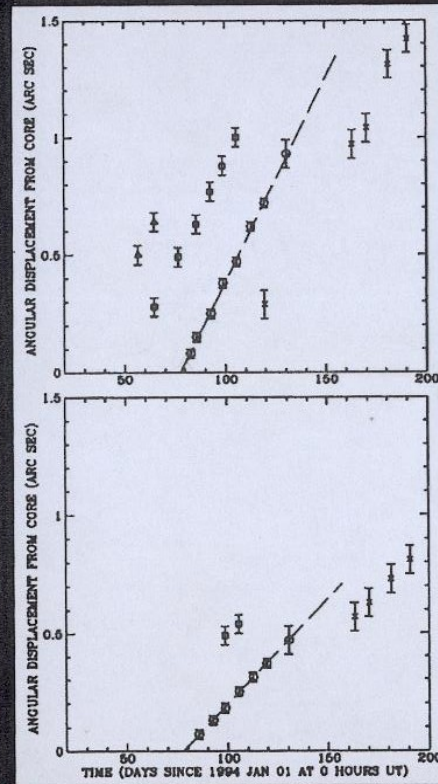
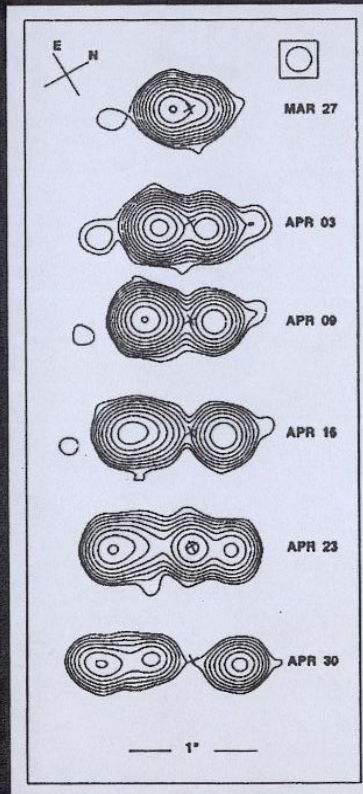
- μ QSO JETS MOVE ON THE SKY $\sim 10^3$ TIMES FASTER THAN QSO JETS

- IN AGN AT $D < 100$ Mpc JETS ARE RESOLVED AT $\sim 50 R_{sh}$ (e.g. M87, Biretta)

PHYSICS: NEED TO STUDY BHs ACROSS ALL MASS SCALES

Relativistic Jets

Relativistic jets
known for many
years in AGN
Spectacular
examples seen
recently in XRBs:
Microquasars



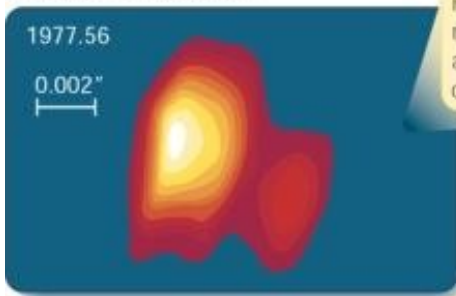
$$\beta_e = \mu_a \frac{D}{c}$$

$$\beta_e = \mu_a \frac{D}{c}$$

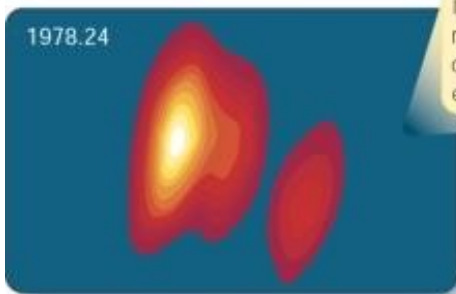
$$\mu_a > 1 !$$

GRS 1915+105: Mirabel & Rodriguez (1995)

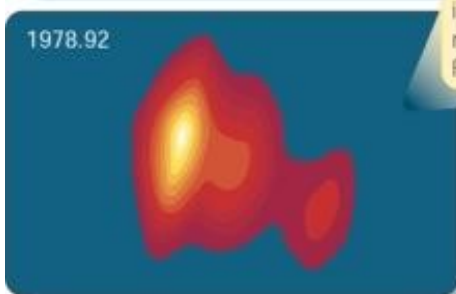
Superluminal Motion



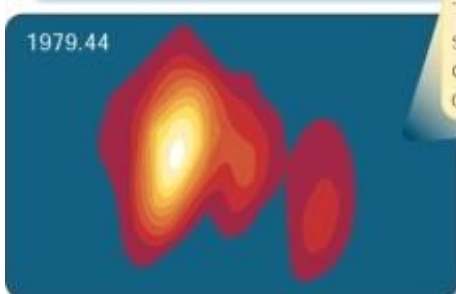
High-resolution radio maps can resolve details as small as a thousandth of a second of arc.



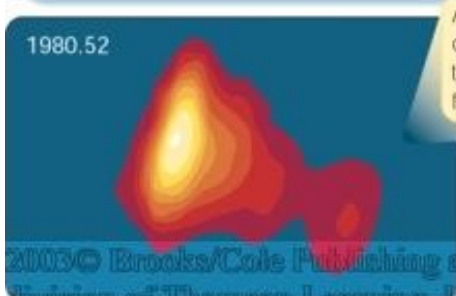
Images of quasar 3C273 recorded over a number of years show gas being ejected...



in the direction of the much longer jet visible in Figure 17-11.



The gas blobs are separating from the quasar at 0.0008 second of arc per year.



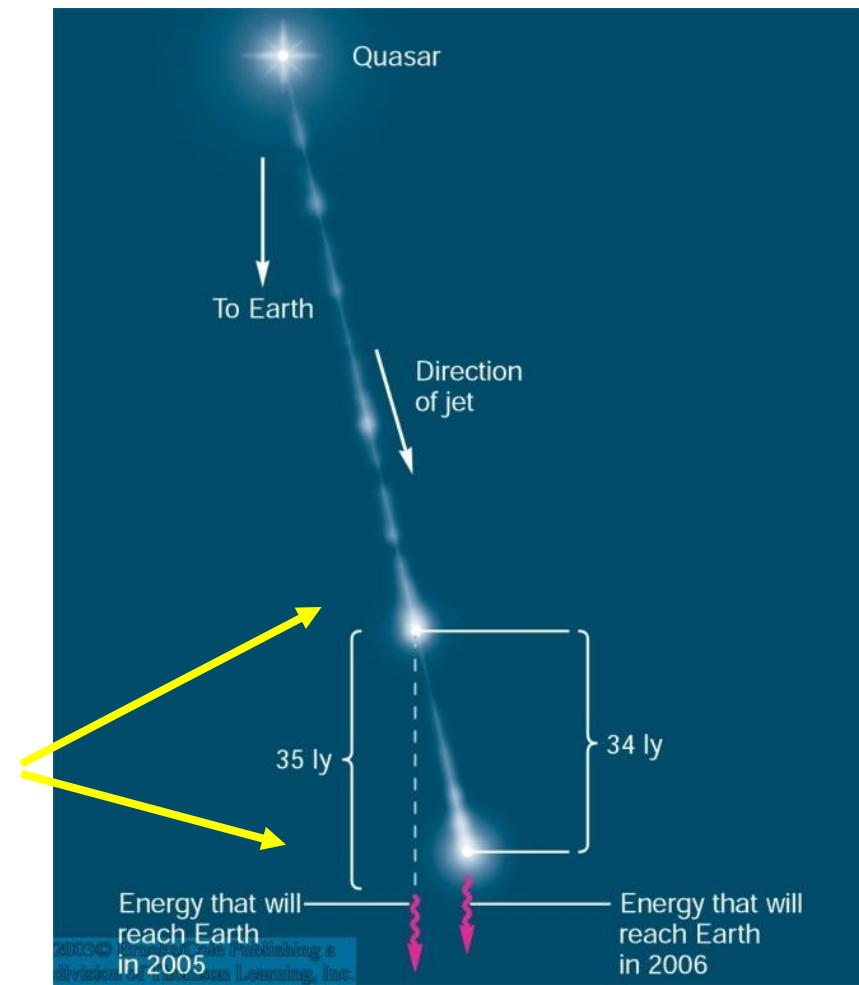
At the distance of the quasar, the gas appears to be moving 12 times faster than light.

Individual radio knots in quasar jets:

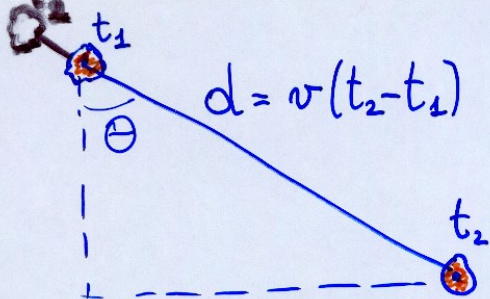
Sometimes apparently moving faster than speed of light!

Light-travel time effect:

Material in the jet is almost catching up with the light it emits



Apparent Superluminal Velocity ⁽⁹⁾



$$t_1' = t_1 + \frac{D}{c}$$

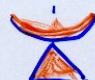
$$t_2' = t_2 + \frac{D}{c} - \frac{d \cos \theta}{c}$$

$$v_{\text{apparent}} = \mu \cdot D = \frac{d \sin \theta}{t_2' - t_1'}$$

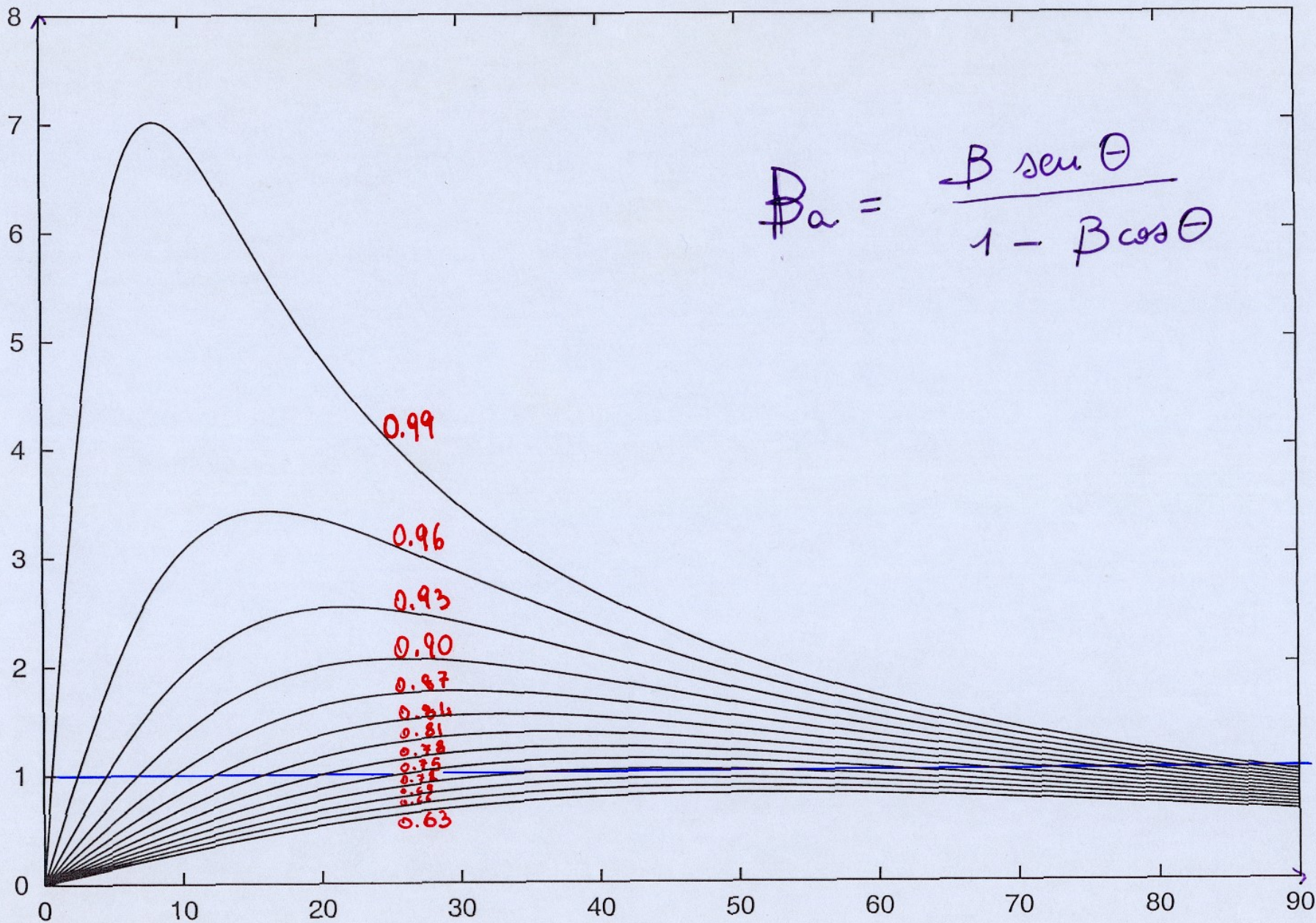
$$\underline{t_2' - t_1'} = (t_2 - t_1) - \frac{v}{c} \cos \theta (t_2 - t_1)$$

$$\Delta t' = \Delta t \left(1 - \frac{v}{c} \cos \theta \right)$$

$$v_{\text{apparent}} = \frac{v (t_2 - t_1) \sin \theta}{(t_2 - t_1) - (t_2 - t_1) \frac{v}{c} \cos \theta}$$


$$\beta_{\text{apparent}} = \frac{\beta \sin \theta}{1 - \beta \cos \theta}$$

β_a



⊖

9:

P

$$v_{\perp}(\text{apparent}) = \frac{v \sin \theta}{1 - v \cos \theta / c}$$

$$\beta_{\perp}(\text{apparent}) = \frac{\beta \sin \theta}{1 - \beta \cos \theta} \quad (5F1)$$

For a fixed β , there is an angle θ that maximizes $\beta_{\perp}(\text{apparent})$. That angle satisfies

$$\frac{\partial \beta_{\perp}(\text{apparent})}{\partial \theta} = 0 = \frac{(1 - \beta \cos \theta) \beta \cos \theta - (\beta \sin \theta)^2}{(1 - \beta \cos \theta)^2}$$

$$\beta \cos \theta - \beta^2 \cos^2 \theta - \beta^2 \sin^2 \theta = 0$$

$$\beta \cos \theta - \beta^2 = 0$$

Thus

$$\beta = \cos \theta \quad (5F2)$$

and

$$\sin \theta = (1 - \cos^2 \theta)^{1/2} = (1 - \beta^2)^{1/2} = \gamma^{-1} \quad (5F3)$$

$$\beta_{\perp}(\text{apparent}) = \frac{\beta \sin \theta}{1 - \beta \cos \theta} \quad (5F1)$$

For a fixed β , there is an angle θ that maximizes $\beta_{\perp}(\text{apparent})$. That angle satisfies

$$\frac{\partial \beta_{\perp}(\text{apparent})}{\partial \theta} = 0 = \frac{(1 - \beta \cos \theta)\beta \cos \theta - (\beta \sin \theta)^2}{(1 - \beta \cos \theta)^2}.$$

$$\beta \cos \theta - \beta^2 \cos^2 \theta - \beta^2 \sin^2 \theta = 0$$

$$\beta \cos \theta - \beta^2 = 0$$

Thus

$$\beta = \cos \theta \quad (5F2)$$

and

$$\sin \theta = (1 - \cos^2 \theta)^{1/2} = (1 - \beta^2)^{1/2} = \gamma^{-1} \quad (5F3)$$

Inserting $\cos \theta = \beta$ and $\sin \theta = \gamma^{-1}$ into our equation for the $\beta_{\perp}(\text{apparent})$ yields the highest apparent transverse speed of a source whose actual speed is β :

Thus

$$\beta = \cos \theta \quad (5F2)$$

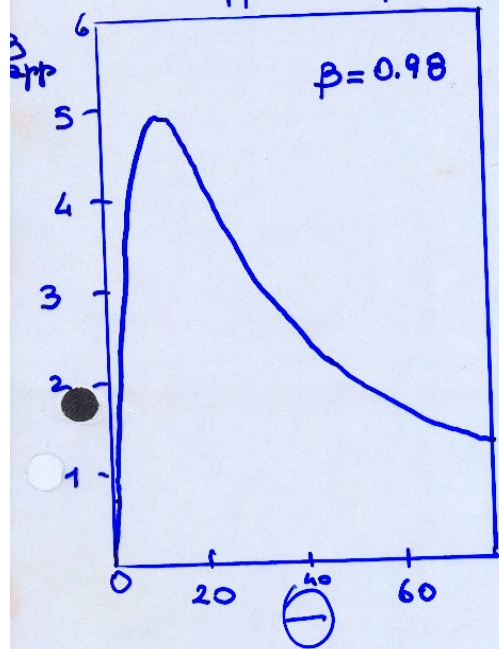
and

$$\sin \theta = (1 - \cos^2 \theta)^{1/2} = (1 - \beta^2)^{1/2} = \gamma^{-1} \quad (5F3)$$

Inserting $\cos \theta = \beta$ and $\sin \theta = \gamma^{-1}$ into our equation for the β_{\perp} (apparent) yields the highest apparent transverse speed of a source whose actual speed is β :

$$\max[\beta_{\perp}(\text{apparent})] = \frac{\beta(1 - \beta^2)^{1/2}}{1 - \beta^2} = \beta\gamma \quad (5F4)$$

Apparent Speed vs. Angle to the line of sight



$$\beta_{app} = \frac{\beta \sin \theta}{1 - \beta \cos \theta}$$

$\beta_{app}^{max} = 4.9$ for $\theta = 11^\circ$ $\cos \theta = 0.98$, $\beta = 0.98$

True in general:

$\cos \theta = \beta \rightarrow \beta_{app}^{max} = \frac{\beta}{\sqrt{1 - \beta^2}}$

for $\beta = 0.999$ ($\gamma = 22$) and $\theta = 2.5^\circ$ $\beta_{app}^{max} = 31$
 $\beta \rightarrow 1$ and $\theta \rightarrow 0$ largest effect! [MAXIMUM]

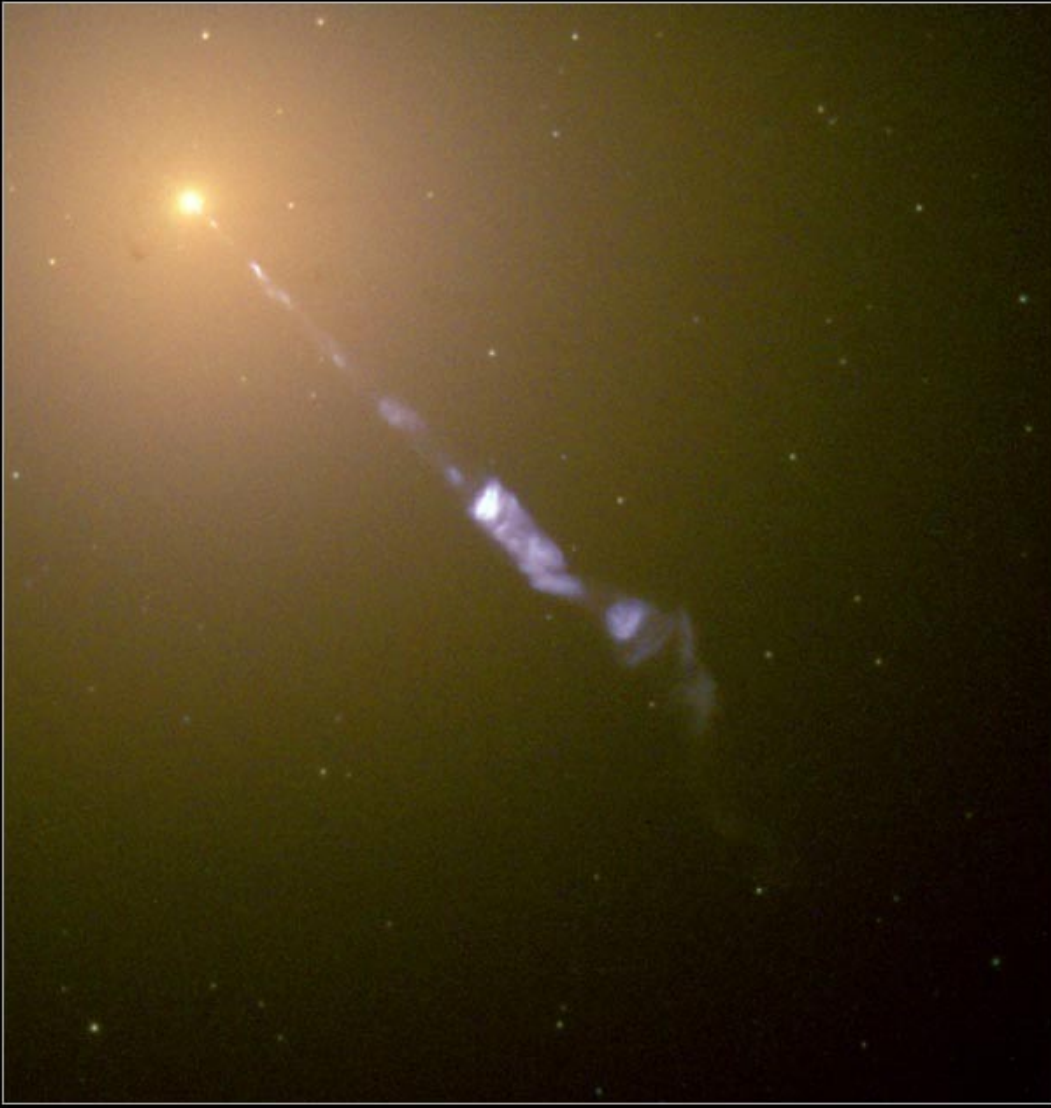
MINIMUM - since que non ----

To have the apparent superluminal motion:

- 1) $\cos \theta = \beta \Rightarrow \beta_{app} \geq 1.1$
- 2) $\beta \geq 0.75$

SUPERLUMINAL MOTIONS IN QSOs & AGN

The M87 Jet



- OBSERVED IN > 30 QSOs & AGN
- IN RADIO & OPTICAL WAVES
- PROPER MOTION SEEN IN YEARS
- V_{app} UP TO $30c$ in blazars
- One sided because of Doppler boosting

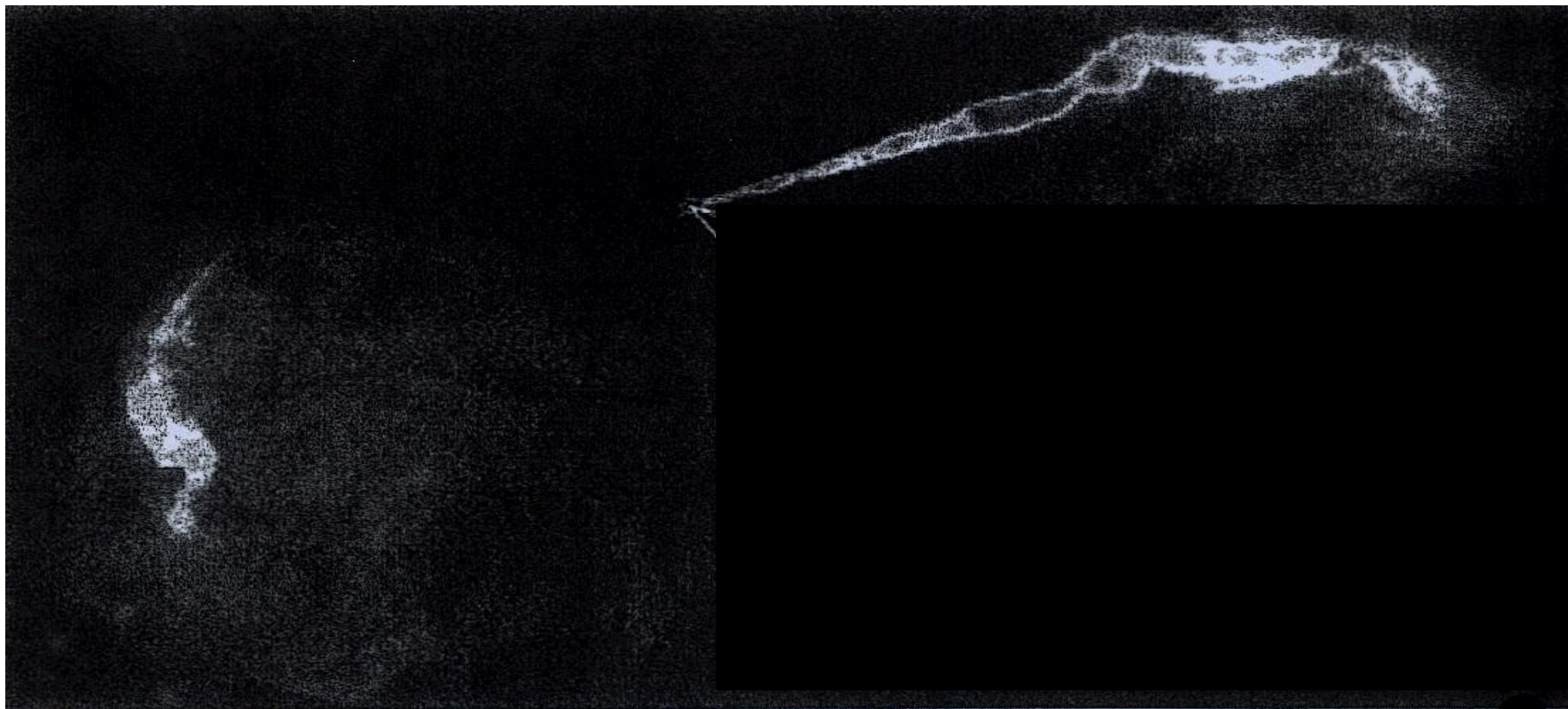


Fig. 1. The jet in the galaxy M87 displays most of the important features of relativistic jets. The approaching northwest jet is Doppler boosted, whereas the southeast one is virtually undetectable because it radiates away from Earth. The lobes, consisting of decelerated jet material, radiate isotropically, and therefore both are visible. The full extent of the source projected on the sky in this image is ~ 80 arc sec or 6 kpc. Because the source is at an angle of $< 19^\circ$ to our line of sight, its deprojected length must be at least 20 kpc. Deep in the core (inset), the jet shows an initial wide opening angle (60°) that decreases with distance from the core. This indicates that the acceleration and collimation region may be resolved. The length of the jet emission in the inset is ~ 0.001 arc sec or 16,000 astronomical units, which is only ~ 250 times the Schwarzschild radius of the central $3 \times 10^9 M_\odot$ black hole. [Images were made with the National Radio Astronomy Observatory's Very Large Array and Very Long Baseline Array and are courtesy of J. Biretta and W. Junor; reprinted with permission from *Nature* (37) copyright (1999) Macmillan Magazines Ltd.]

Receding

$$f_a = \frac{f_0 \sin \theta}{1 - \beta \cos \theta}$$

$$f_r = \frac{f_0 \sin \theta}{1 + \beta \cos \theta}$$

Approaching

DOPPLER BOOSTING

$$\lambda_a = \frac{\lambda}{\gamma(1 - \beta \cos \theta)}$$

$$\lambda_r = \frac{\lambda}{\gamma(1 + \beta \cos \theta)}$$

$$S_a = S_0 \left[\frac{1}{\gamma(1 - \beta \cos \theta)} \right]^{k-h}$$

$$S_r = S_0 \left[\frac{1}{\gamma(1 + \beta \cos \theta)} \right]^{k-h}$$

$$\gamma = \frac{1}{\sqrt{1 - \beta^2}}$$

$$\text{Doppler factor} = \frac{1}{\gamma(1 - \beta \cos \theta)}$$

$$\beta \ll 1 \quad \text{Doppler factor} \approx 1 + \beta \cos \theta$$

$$\lambda = \frac{\lambda_0}{\gamma} \cdot \frac{1}{(1 - \beta \cos \theta)} = \frac{\lambda_0 \sqrt{1 - \beta^2}}{(1 - \beta \cos \theta)} \quad (*)$$

$$\gamma = \frac{1}{\sqrt{1 - \beta^2}} \quad \beta = \frac{v}{c}$$

$$\beta \approx 0$$

$$f = f(0) + \left. \frac{\partial f}{\partial \beta} \right|_{\beta=0} (\beta - 0)$$

$$f(0) = \lambda_0$$

$$f' = \lambda_0 \left[\frac{\frac{1}{2} \cdot 2 \beta (1 - \beta^2)^{-1/2} (1 - \beta \cos \theta) - (1 - \beta^2)^{1/2} (-\cos \theta)}{(1 - \beta \cos \theta)^2} \right]$$

$$\left. \frac{df}{d\beta} \right|_{\beta=0} = \cos \theta \cdot \lambda_0$$

$$\nu = \nu_0 + \nu_0 \cos \theta \beta = \nu_0 \left(1 + \frac{\nu}{c} \cos \theta \right)$$

$$\nu - \nu_0 = \nu_0 \frac{\nu}{c} \cos \theta$$

$$\nu = \nu_0 [\beta \cos \theta + 1]$$

$$\frac{\Delta \nu}{\nu_0} = \frac{\nu}{c} \cos \theta$$

$$\frac{\nu - \nu_0}{\nu_0} = \frac{\Delta \nu}{\nu_0} = \frac{\Delta \lambda}{\lambda} \left(\frac{c}{\lambda} - \frac{c}{\lambda_0} \right) = \frac{\Delta \lambda}{\lambda} \left(\frac{c \lambda_0 - c \lambda}{\lambda \lambda_0} \right) = \frac{\lambda_0 - \lambda}{\lambda}$$

$$(*) \quad \nu - \nu_0 = \frac{\nu_0 \sqrt{1 - (\frac{v}{c})^2}}{(1 - \frac{v}{c} \cos \theta)} - \nu_0$$

$$\frac{\Delta \nu}{\nu_0} = \frac{\sqrt{1 - (\frac{v}{c})^2}}{(1 - \frac{v}{c} \cos \theta)} - 1$$

Superluminal motions

$$\lambda_o = M_{app} \frac{D}{c} = \frac{\beta \sin \theta}{(1 - \beta \cos \theta)}$$

$$\lambda_r = M_{rec} \frac{D}{c} = \frac{\beta \sin \theta}{1 + \beta \cos \theta}$$

$$\beta \cos \theta = \frac{M_{app} - M_{rec}}{M_{app} + M_{rec}}$$

$$\theta = \tan^{-1} \left[1.16 \times 10^{-2} \left(\frac{M_{app} M_{rec}}{M_{app} - M_{rec}} \right) D \right]$$

Doppler Boosting

$$S_a = \frac{L_a}{L_o} = \gamma^{-1} (1 - \beta \cos \theta)^{-1}$$

$$S_r = \frac{L_r}{L_o} = \gamma^{-1} (1 + \beta \cos \theta)^{-1}$$

$$\frac{S_a}{S_o} = S_a^{k-d} ; \frac{S_r}{S_o} = S_r^{k-d}$$

$$\frac{S_a}{S_r} = \left(\frac{1 + \beta \cos \theta}{1 - \beta \cos \theta} \right)^{k-d}$$

Appendix A: Lower limit of β

The ratio of observed flux densities from a twin pair of optically-thin emitting jets (approaching and receding), with intrinsic velocity βc and angle between the ejection and the line of sight θ , is:

$$\frac{S_a}{S_r} = \left(\frac{1 + \beta \cos \theta}{1 - \beta \cos \theta} \right)^{k-\alpha}, \quad (\text{A1})$$

where k is 2 for a continuous jet and 3 for discrete condensations, and α is the spectral index of the source.

If we assume that the twin jets are gaussian like, then the density flux is:

$$S = \frac{\text{Peak}(\text{mJy/beam})\Omega_{\text{source}}}{\Omega_{\text{beam}}} \quad (\text{A2})$$

where Ω_{source} and Ω_{beam} are the solid angles of source and beam. Hence, the ratio of the flux densities of the twin components can be expressed as:

$$\frac{S_a}{S_r} = \frac{\text{Peak}_a(\text{mJy/beam})\Omega_{\text{source}_a}}{\text{Peak}_r(\text{mJy/beam})\Omega_{\text{source}_r}} \quad (\text{A3})$$

If in a map we deal with the approaching jet only, we can set as upper limit for the Peak_r the 3σ level of the map. An upper limit for Ω_r is Ω_a , because the receding component is expected to be compressed with respect to the approaching one. Then we can write:

$$\frac{S_a}{S_r} > \frac{\text{Peak}_a(\text{mJy/beam})}{3\sigma} \quad (\text{A4})$$

Combining eq. A1 and eq. A4 we obtain:

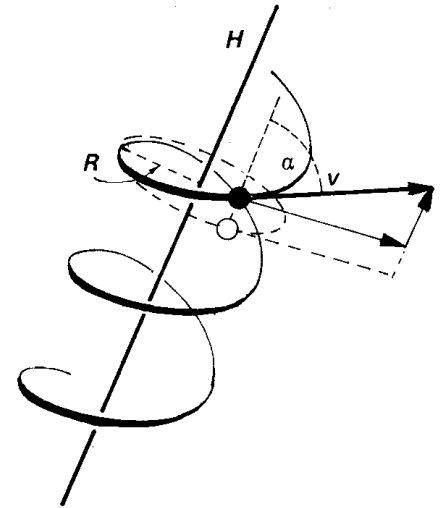
$$\beta \cos \theta > \frac{\left(\frac{\text{Peak}_a}{3\sigma} \right)^{\frac{1}{k-\alpha}} - 1}{\left(\frac{\text{Peak}_a}{3\sigma} \right)^{\frac{1}{k-\alpha}} + 1} \quad (\text{A5})$$

Relativistic electrons in a magnetic field

$$E = \gamma m_e c^2 \quad \gamma = \frac{1}{\sqrt{1 - \frac{v^2}{c^2}}} \quad \gamma \gg 1$$

For one electron, max frequency $\propto \gamma^2$

Electron energy distribution is a power law: $N(E) dE = k E^{-p} dE$



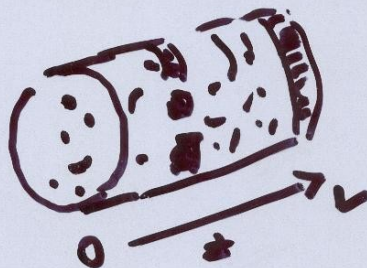
Radiative Transfer Equation

R.T: process of transmission of the electro-magnetic radiation through the atmosphere

$$\frac{dI}{dz} = \underset{\substack{\uparrow \\ \text{emissivity}}}{J} - \underset{\substack{\uparrow \\ \text{absorption coefficient}}}{K} I$$

$$I(\theta, \varphi, z, \nu)$$

Intensity in $\text{erg cm}^{-2} \text{ster}^{-1} \text{s}^{-1}$



Flux Density

$$S = \int I d\Omega$$

$$d\Omega = \sin\theta d\theta d\varphi$$

$$0 < \theta < \frac{\theta_{\text{SOURCE}}}{2}$$

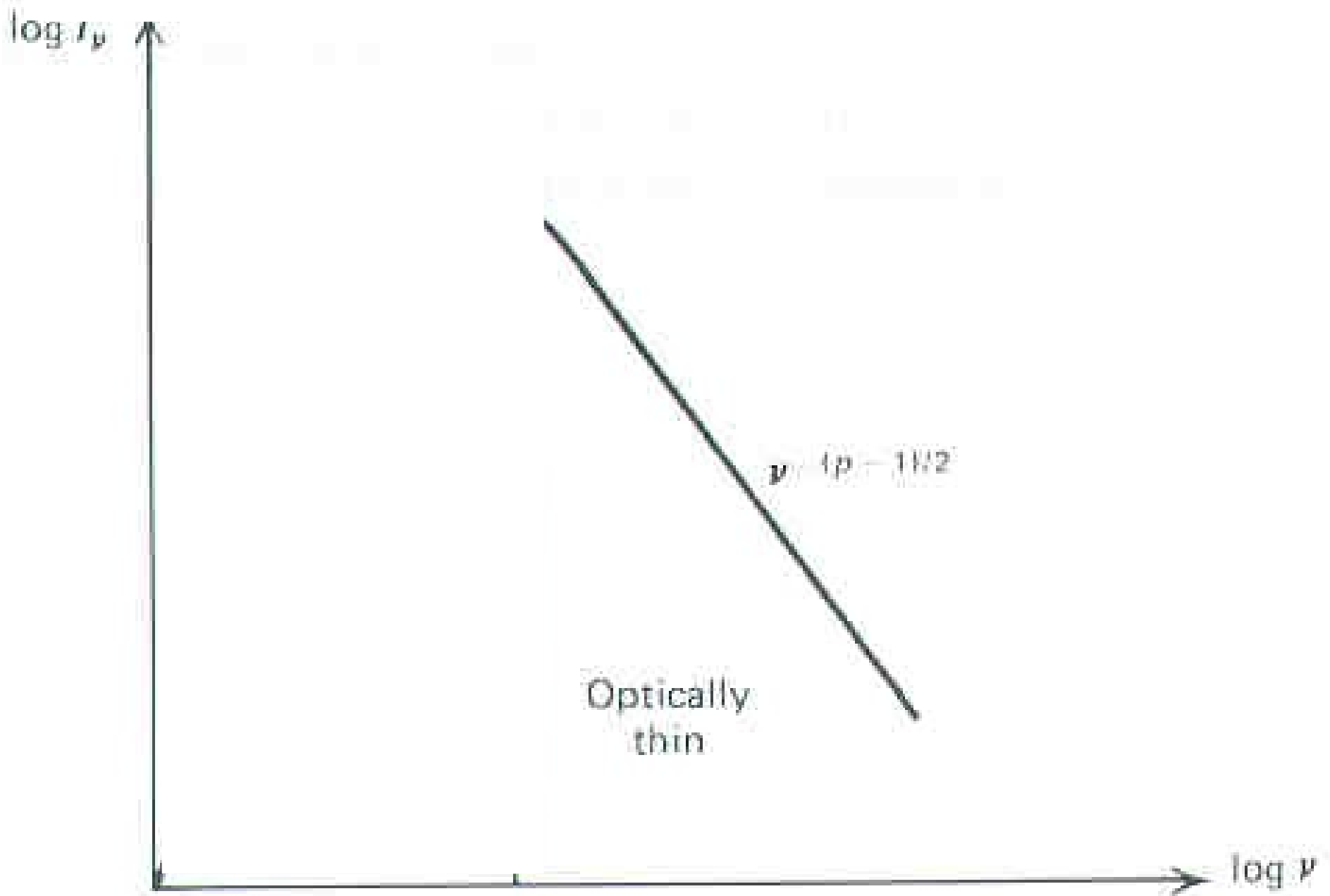
$$0 < \varphi < 2\pi$$

$$N(E)dE = CE^{-p}dE$$

In this case, we have

$$S(\nu) \propto \nu^{-\frac{p-1}{2}}$$

Flux density vs frequency



Synchrotron Self-absorption

According to the principle of detailed balance, to every emission process there is a corresponding absorption process – in the case of synchrotron radiation, this is known as *synchrotron self-absorption*.

Suppose a source of synchrotron radiation has a power law spectrum, $S_\nu \propto \nu^{-\alpha}$, where the spectral index $\alpha = (p - 1)/2$. Its *brightness temperature* is defined to be $T_b = (\lambda^2/2k)(S_\nu/\Omega)$, and is proportional to $\nu^{-(2+\alpha)}$, where S_ν is its flux density and Ω is the solid angle it subtends at the observer at frequency ν . We recall that brightness temperature is the temperature of a black-body which would produce the observed surface brightness of the source at the frequency ν in the Rayleigh-Jeans limit, $h\nu \ll kT_e$. Thus, at low enough frequencies, the brightness temperature of the source may approach the kinetic temperature of the radiating electrons. When this occurs, self-absorption becomes important since thermodynamically the source cannot emit radiation of brightness temperature greater than its kinetic temperature.

Synchrotron Self-absorption

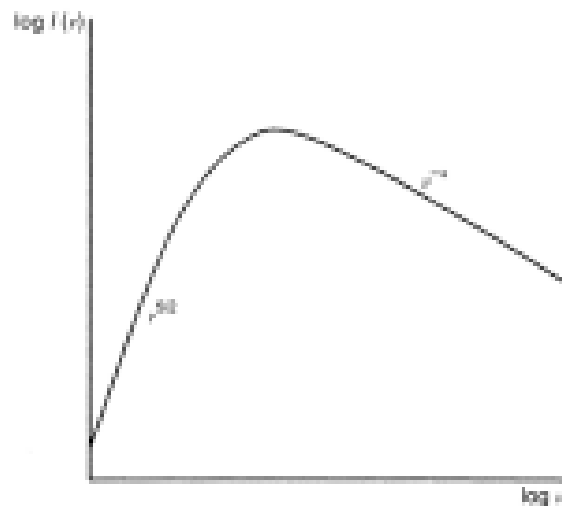
The important point is that the *effective temperature* of the particles now becomes a function of their energies. Since $\gamma \approx (\nu/\nu_g)^{1/2}$,

$$T_e \approx (mec^2/3k)(\nu/\nu_g)^{1/2}. \quad (40)$$

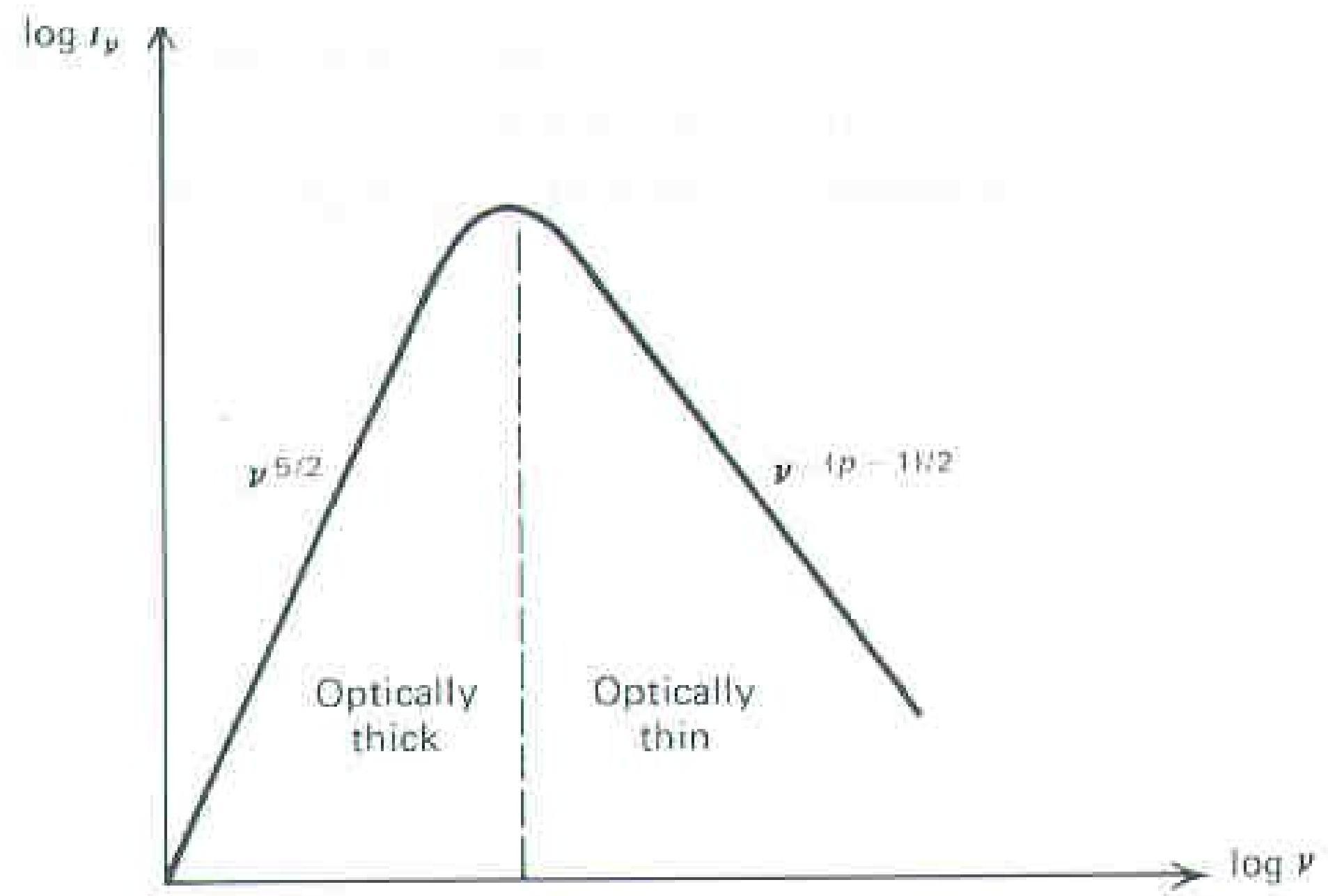
For a self-absorbed source, the brightness temperature of the radiation must be equal to the kinetic temperature of the emitting particles, $T_b = T_e$, and therefore, in the Rayleigh-Jeans limit,

$$S_\nu = \frac{2kT_e}{\lambda^2} \Omega = \frac{2m_e}{3\nu_g^{1/2}} \Omega \nu^{5/2} \propto \frac{\theta^2 \nu^{5/2}}{B^{1/2}}, \quad (41)$$

where Ω is the solid angle subtended by the source, $\Omega \approx \theta^2$. Spectra of roughly this form are found at radio, centimetre and millimetre wavelengths from the nuclei of active galaxies and quasars.



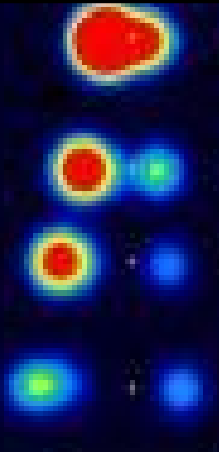
Flux density (Jy)



TRANSIENT JETS

STEADY JETS

GRS 1915+105



Mirabel & Rodriguez 1994

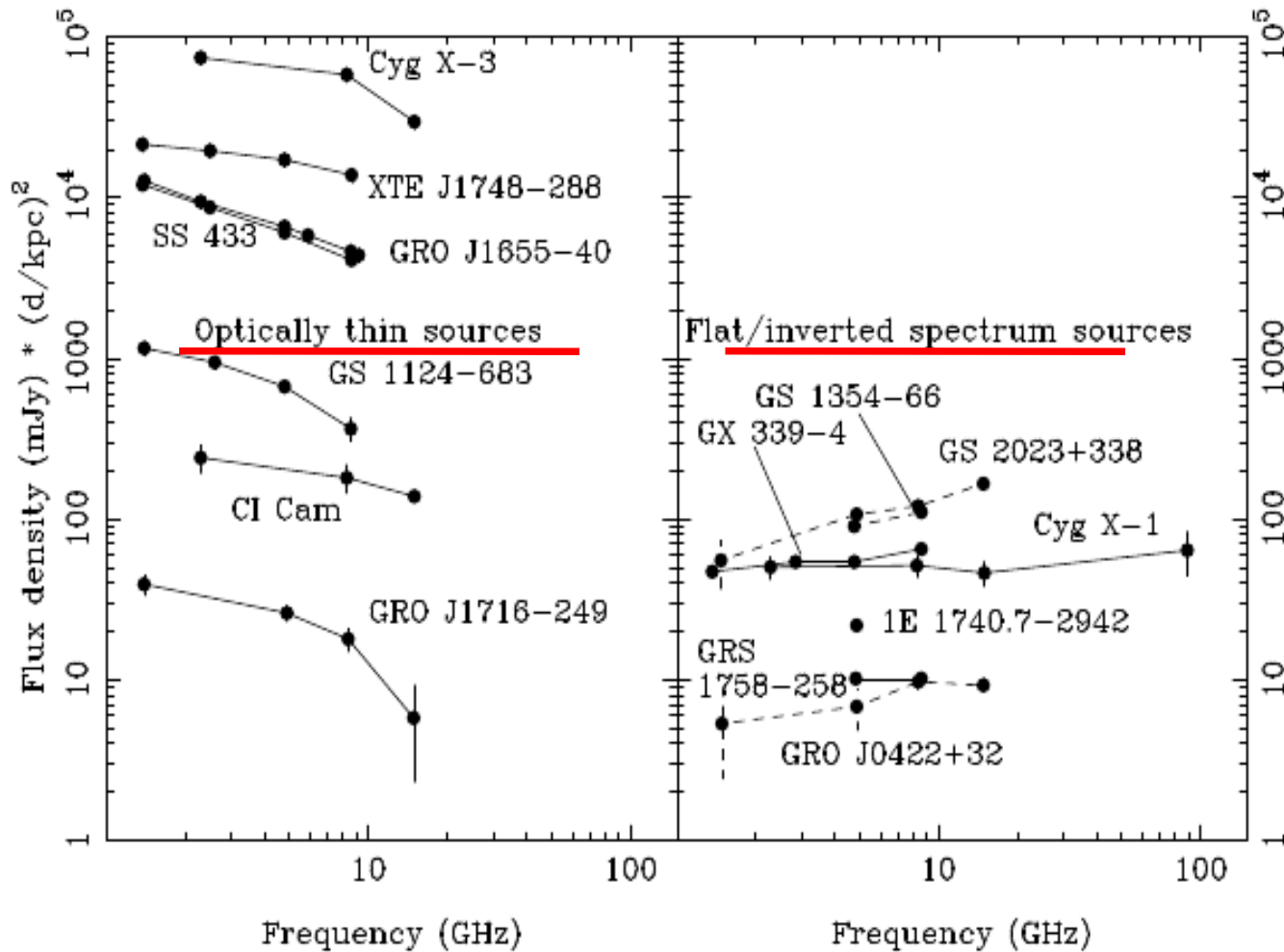
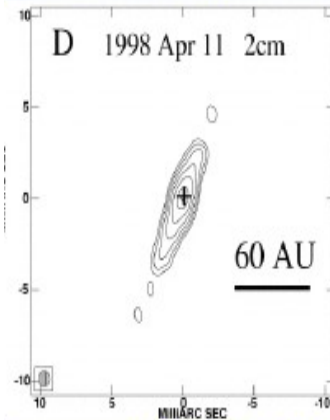


Figure 4. Optically thin (i.e. spectral index $\alpha < 0$) radio spectra from several radio-bright X-ray binaries which were *not* in the Low/Hard X-ray state at the time of the observations, compared with the flat/inverted spectra of the seven sources in Figs 1 & 4 (for the transients, the later, i.e. most inverted, spectra are plotted). As well as the different spectral indices (the optically thin sources all have $-1 \leq \alpha \leq -0.2$, the source in the Low/Hard state all have $0.0 \leq \alpha \leq 0.6$), note also the much wider range of fluxes observed from optically thin emission.

GRS 1915+105

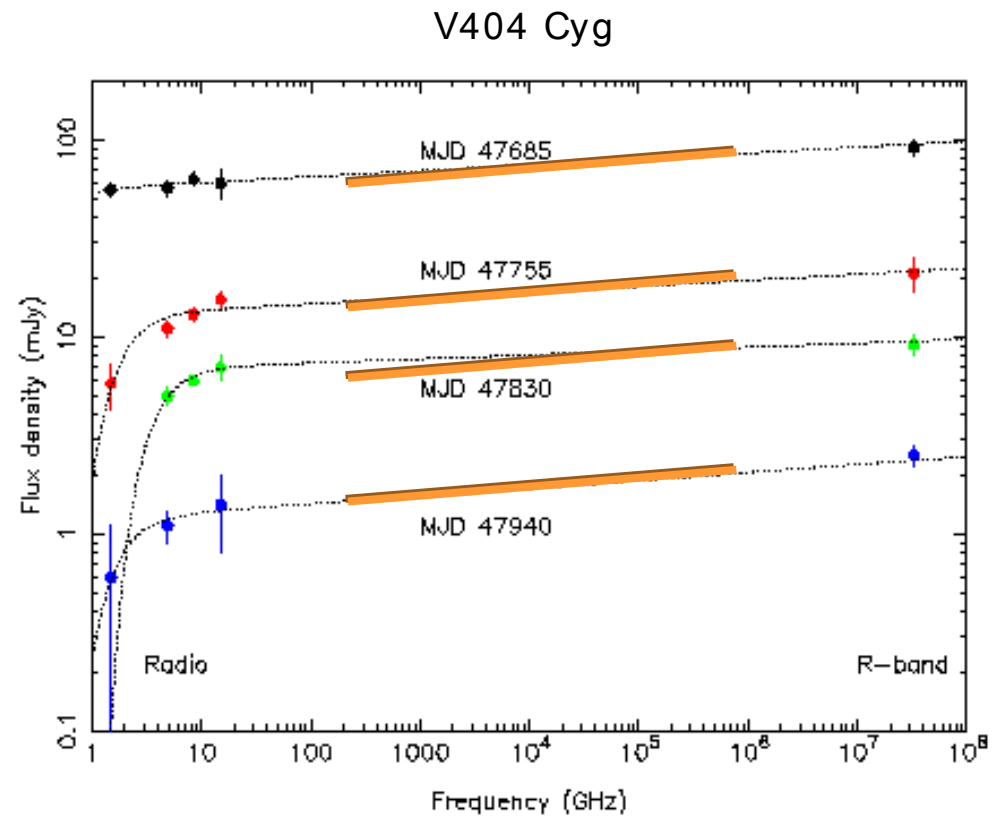


Dhawan et al. 2000

Fender et al. 2001, 2004, 2006

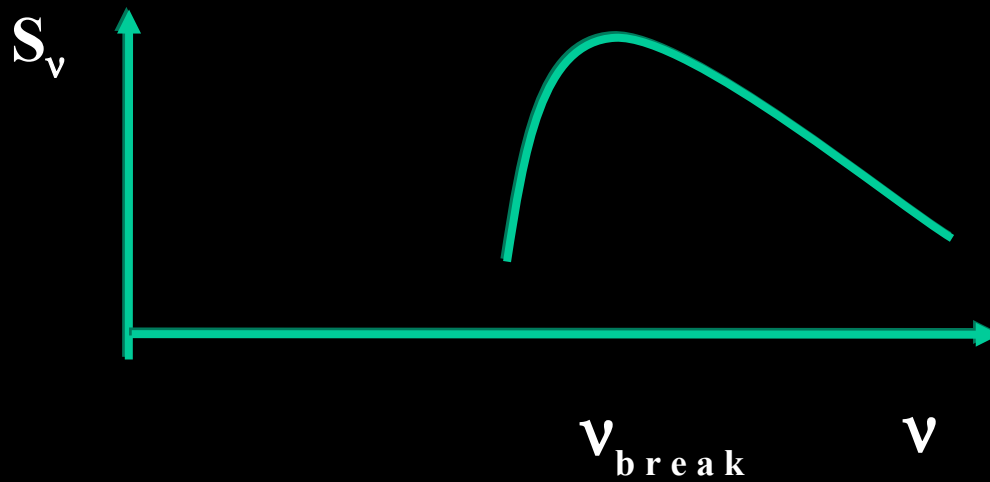
The radio-optical spectrum of XRBs

- Radio-to-NIR spectrum is flat in the hard state.



(Fender
2000)

RADIO SPECTRUM: WHY IS IT “FLAT” ?



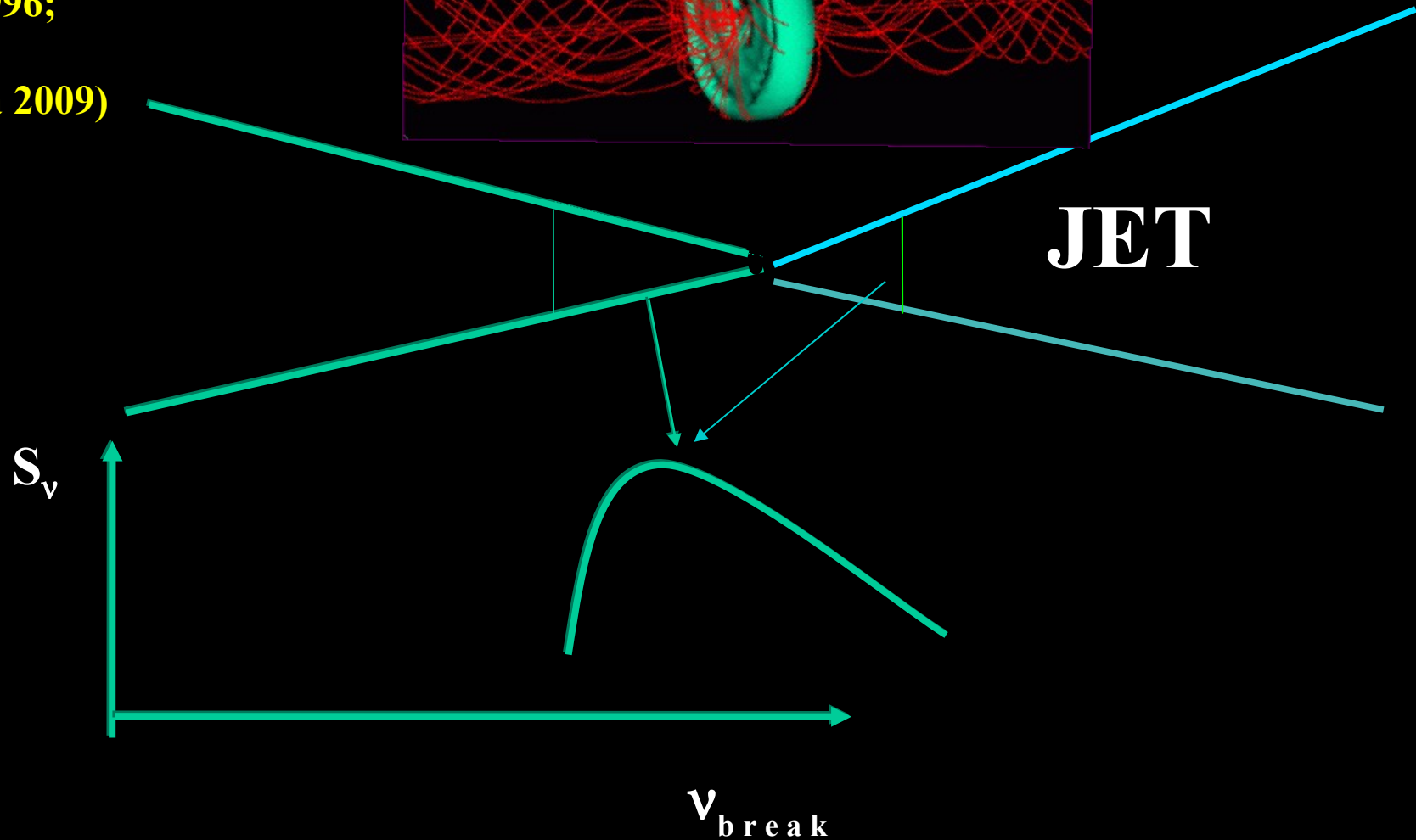
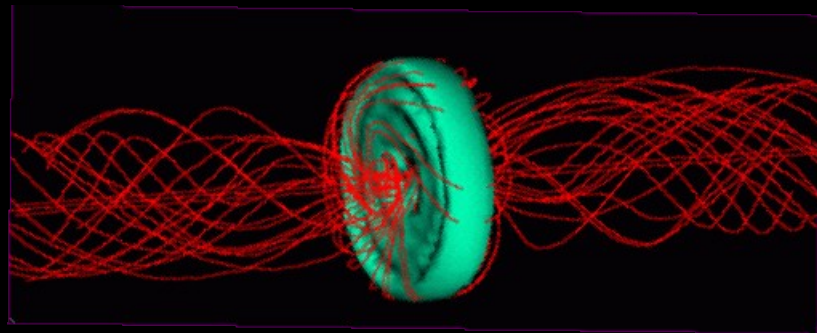
$$v_{\text{peak}} \approx 3.2 \times 10^7 \sin \theta \left(\frac{E_0}{1 \text{ MeV}} \right)^{(2\delta - 2)/(\delta + 4)} \\ \times \left[8.7 \times 10^{-12} \frac{\delta - 1}{\sin \theta} NL \right]^{2/(\delta + 4)} B^{(\delta + 2)/(\delta + 4)},$$

$$n(E) = KE^{-\delta},$$

where K is related to N , the number of electrons per cubic centimeter

Dulk (1985), *Ann. Rev. Astronomy & Astrophysics*, 23, 183

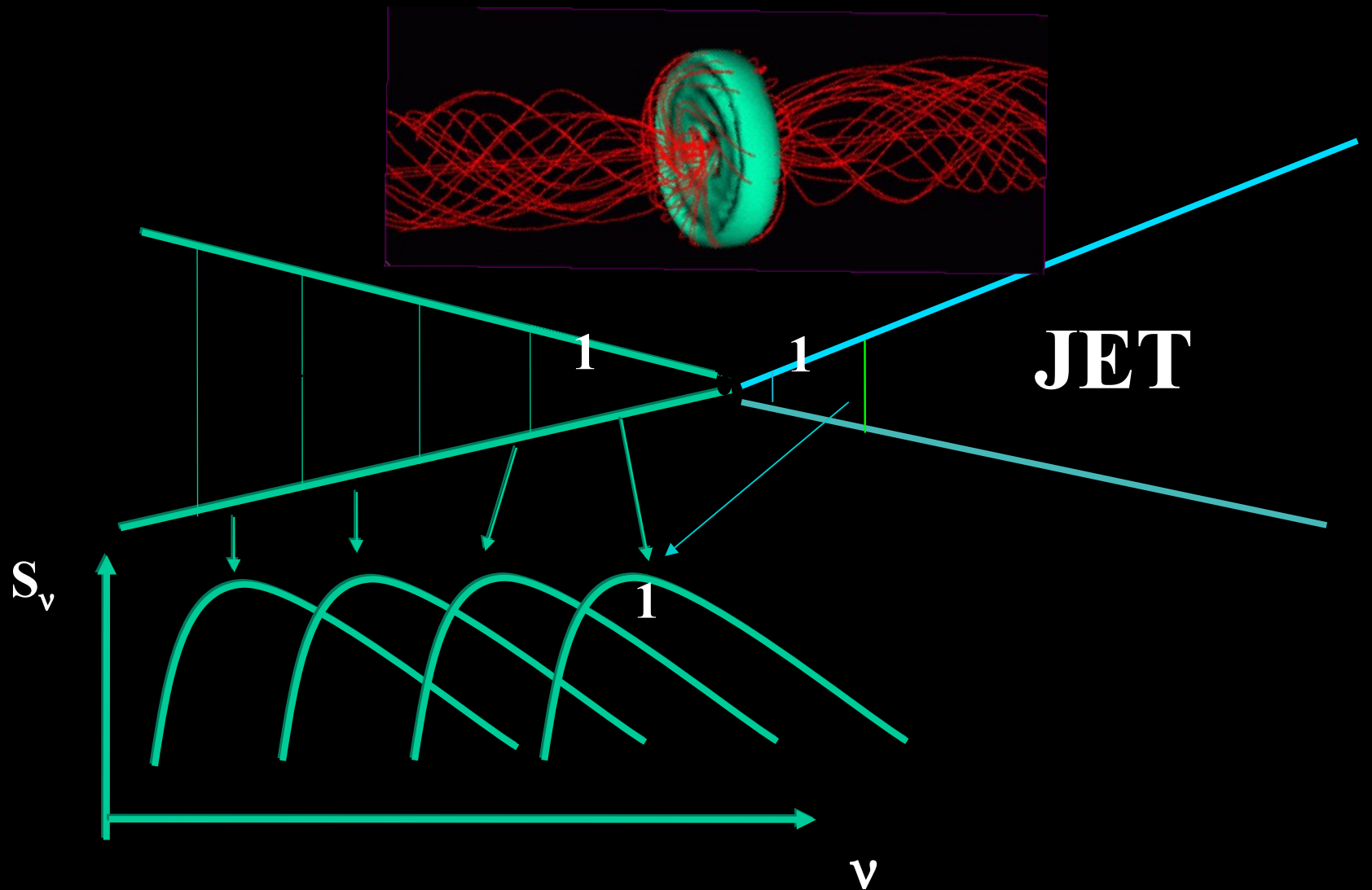
Blandford & Konigl 1979;
Hjellming & Johnston 1988;
Falcke et al. 1996;
Kaiser 2006;
Pe'er & Casella 2009)



Change of the plasma conditions along the jet:

decay of the magnetic field

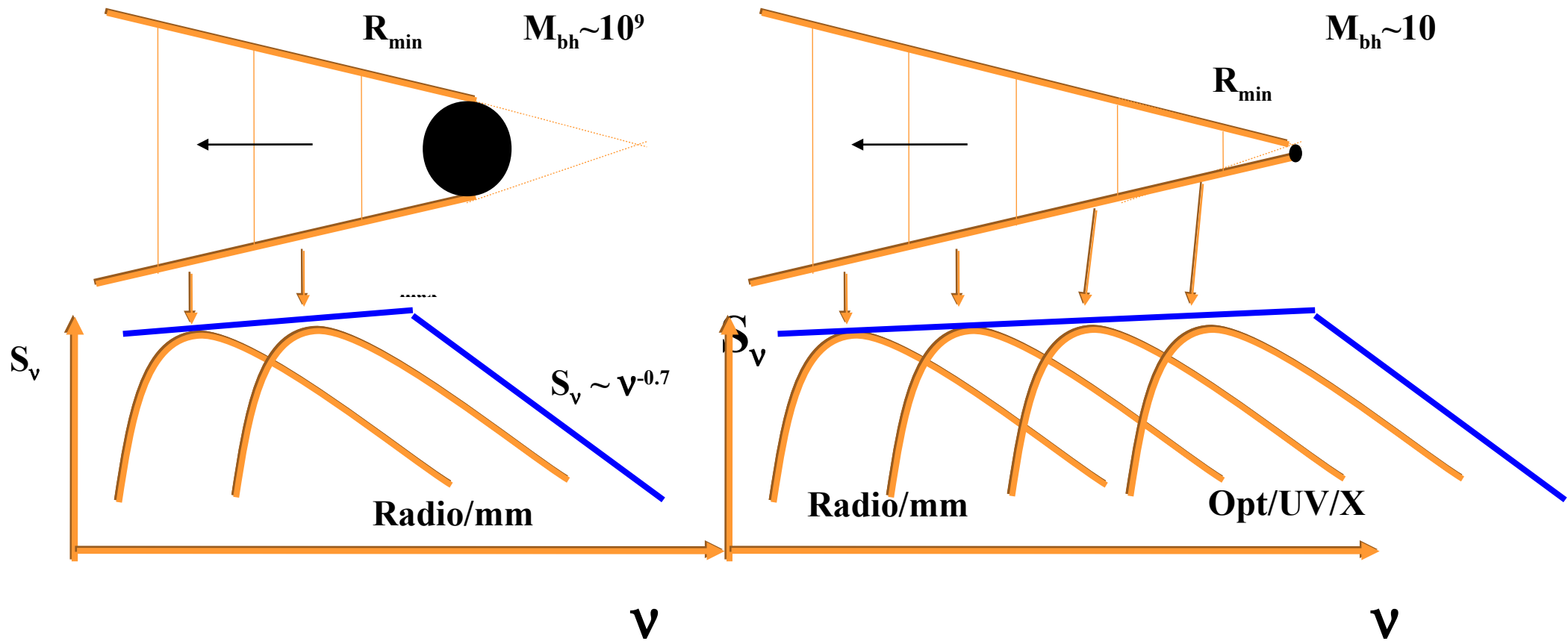
change in the electron energy distribution



dependence of the "break" frequency on the changing plasma conditions along the jet

Blandford & Konigl 1979;

Hjellming & Johnston 1988; Falcke et al. 1996; Kaiser 2006; Pe'er & Casella 2009



turnover frequency in stellar black holes $>$ blazars ($B_{XRB} \gg B_{AGN}$)

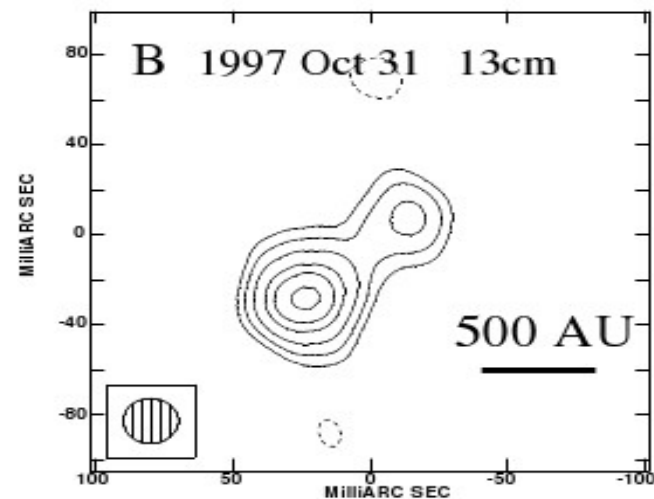
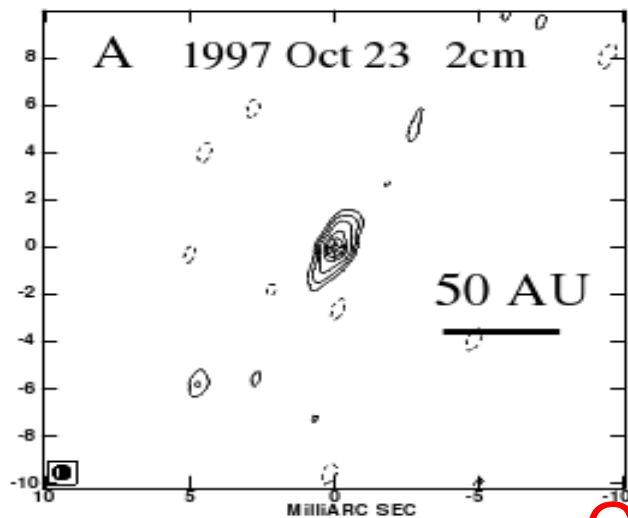
Steady Radio Jet

slow velocity
 $\sim 0.1 c$

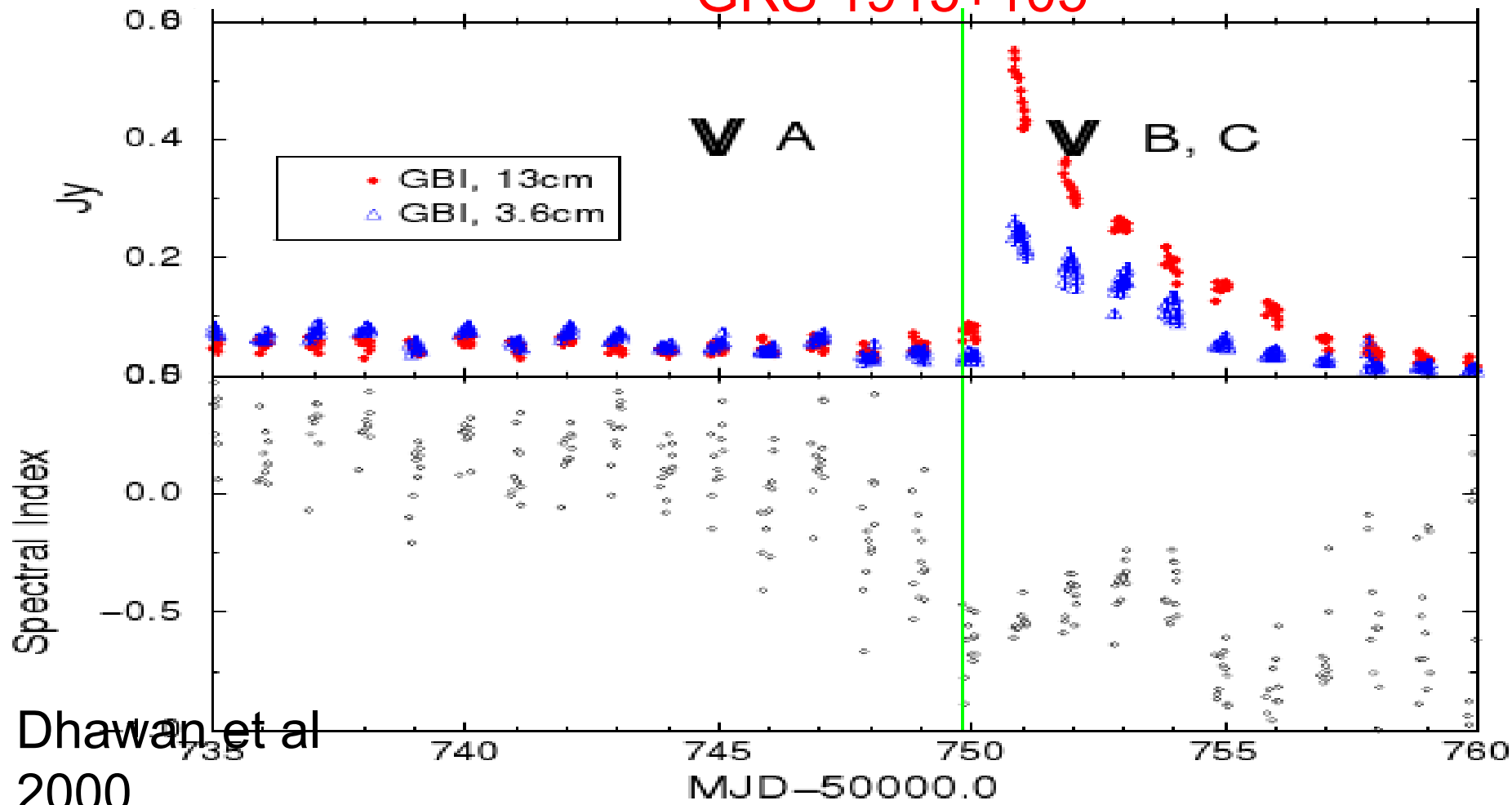
Dhawan et al.
2000

Continuous
conical jet
centered on the
system,
flat radio
spectrum

Compact jets



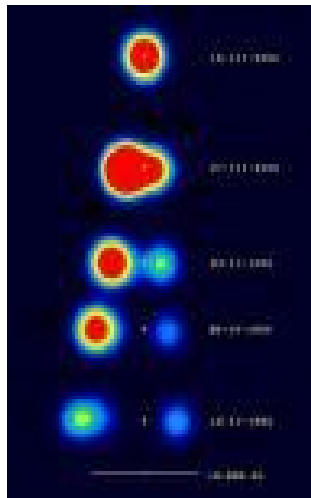
GRS 1915+105



Two distinct radio emission states

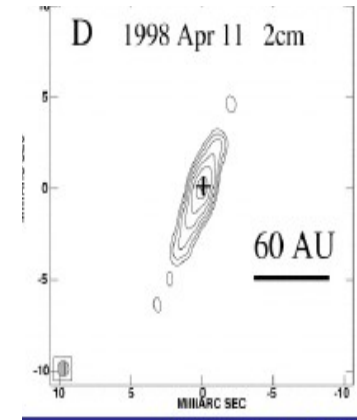
radio emission **attached to**.....

and **detached from** the center



GRS 1915+105

Mirabel .& Rodrigez 1994

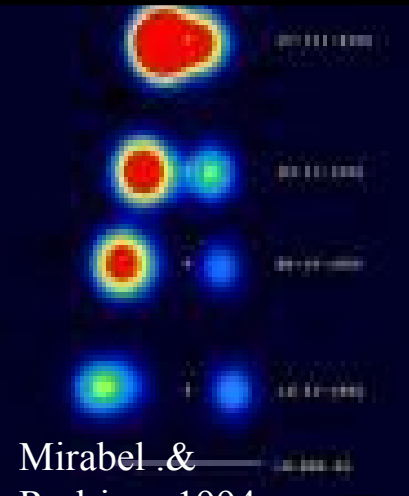


GRS 1915+105

Dhawan et al.
2000

TRANSIENT JETS

STEADY JETS



Mirabel & Rodriguez 1994

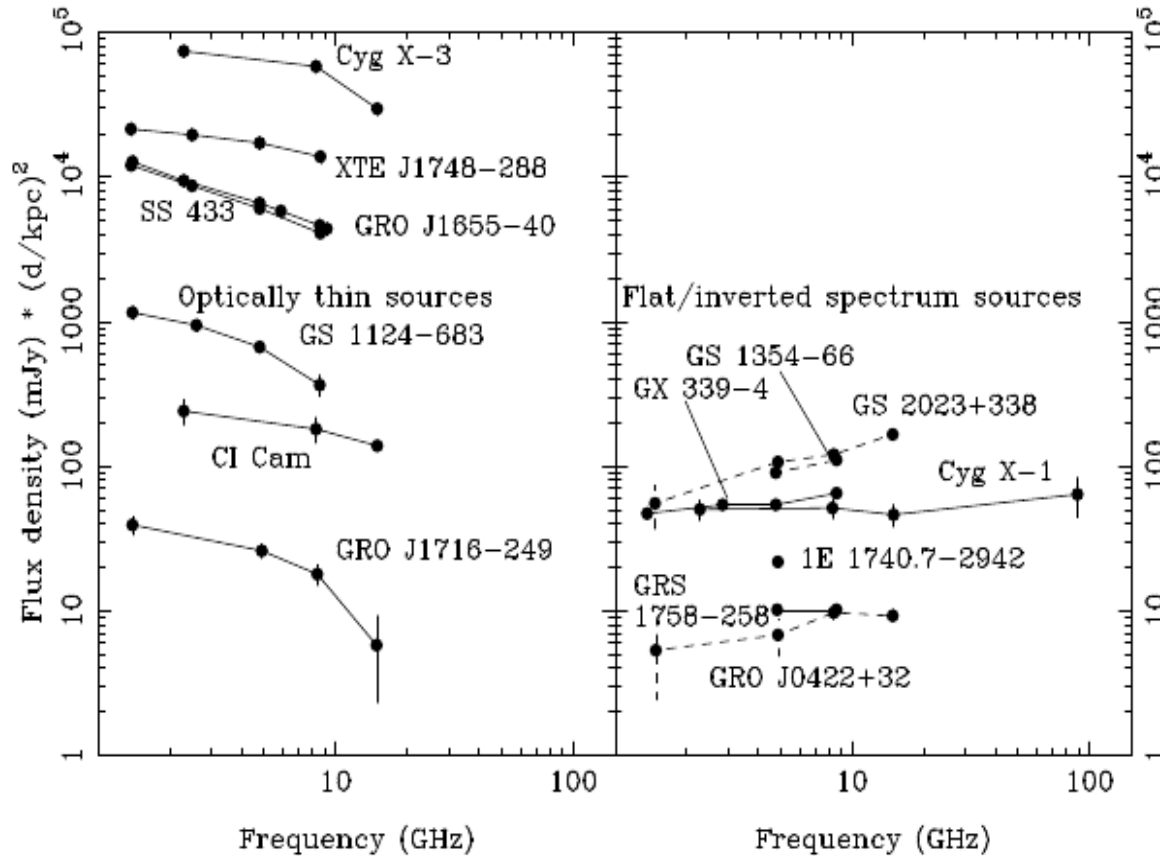
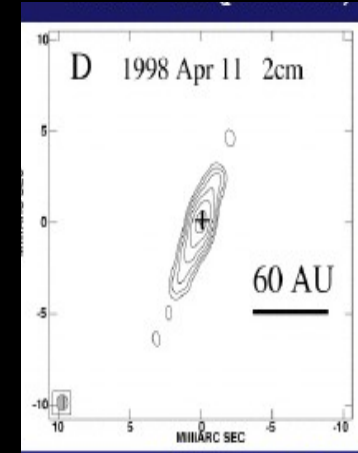


Figure 4. Optically thin (i.e. spectral index $\alpha < 0$) radio spectra from several radio-bright X-ray binaries which were *not* in the Low/Hard X-ray state at the time of the observations, compared with the flat/inverted spectra of the seven sources in Figs 1 & 4 (for the transients, the later, i.e. most inverted, spectra are plotted). As well as the different spectral indices (the optically thin sources all have $-1 \leq \alpha \leq -0.2$, the source in the Low/Hard state all have $0.0 \leq \alpha \leq 0.6$), note also the much wider range of fluxes observed from optically thin emission.



Dhawan et al. 2000

X-ray State

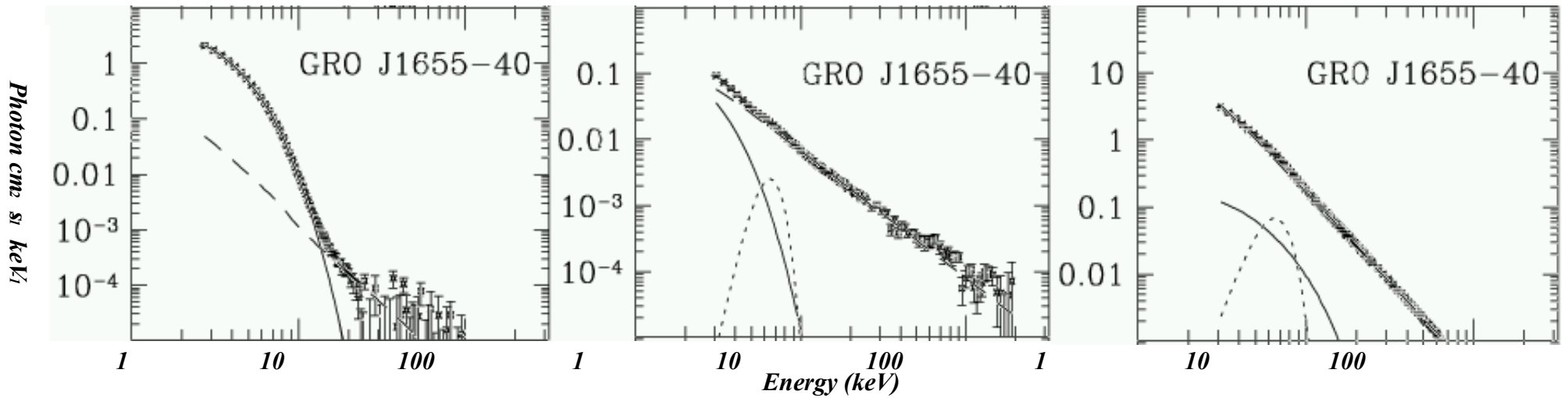
**Steep
Power-law
State**

X-ray State

Low Hard

Accretion states

Energy spectra from McClintock & Remillard (2006)



High

(thermal dominated)

~ 1 – 2 keV disc + PL tail

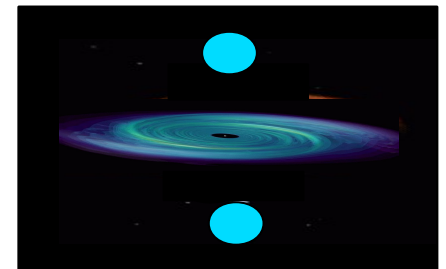
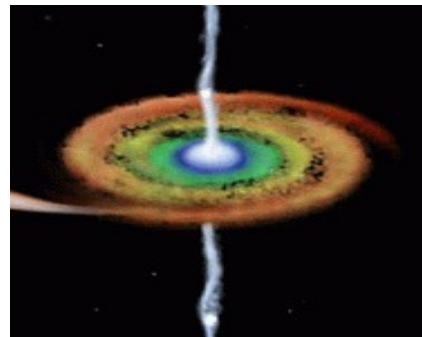
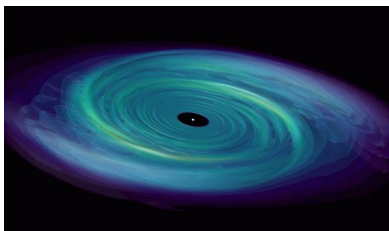
Low/Hard

Hard PL ($\Gamma \sim 1.5 - 2$) dominant, disc absent or truncated, radio jet emission. Least luminous.

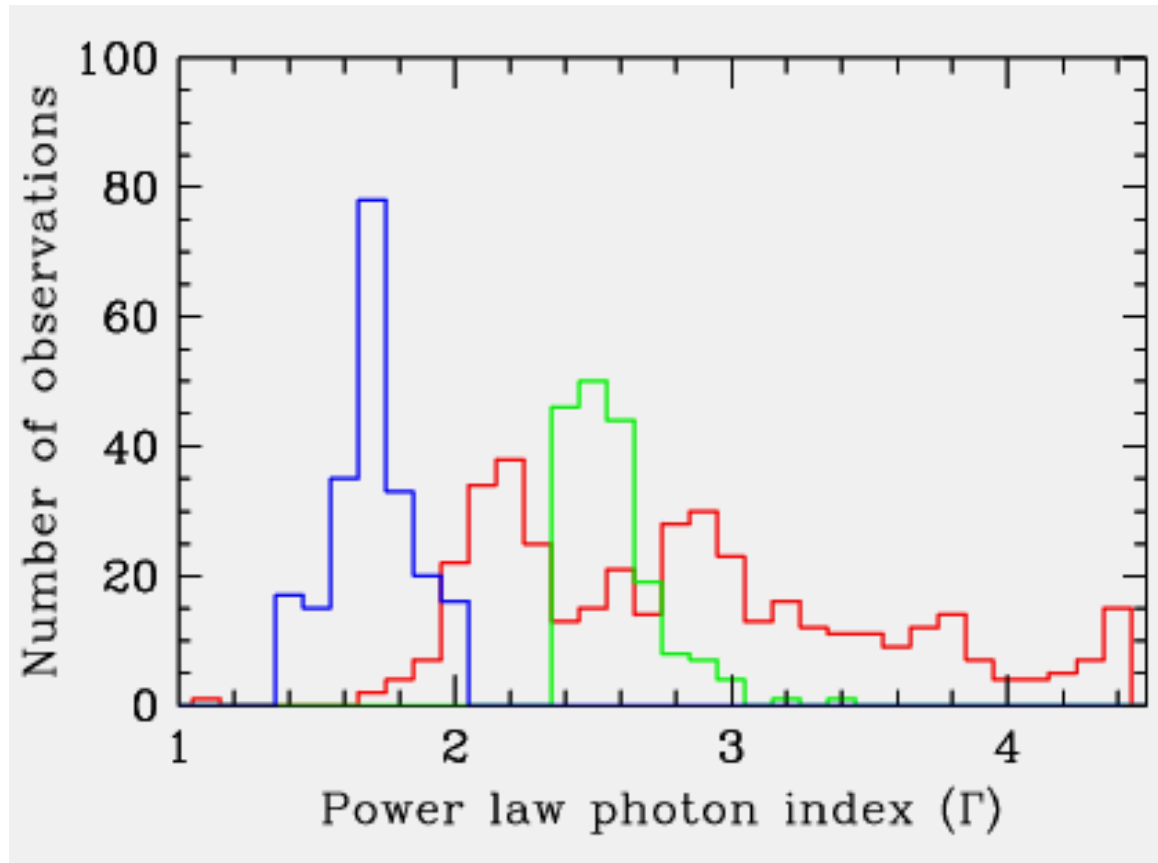
Very High

(steep power-law)

Soft PL ($\Gamma > 2.5$) plus some hot disc emission. Most luminous.



Distributions in Photon Index



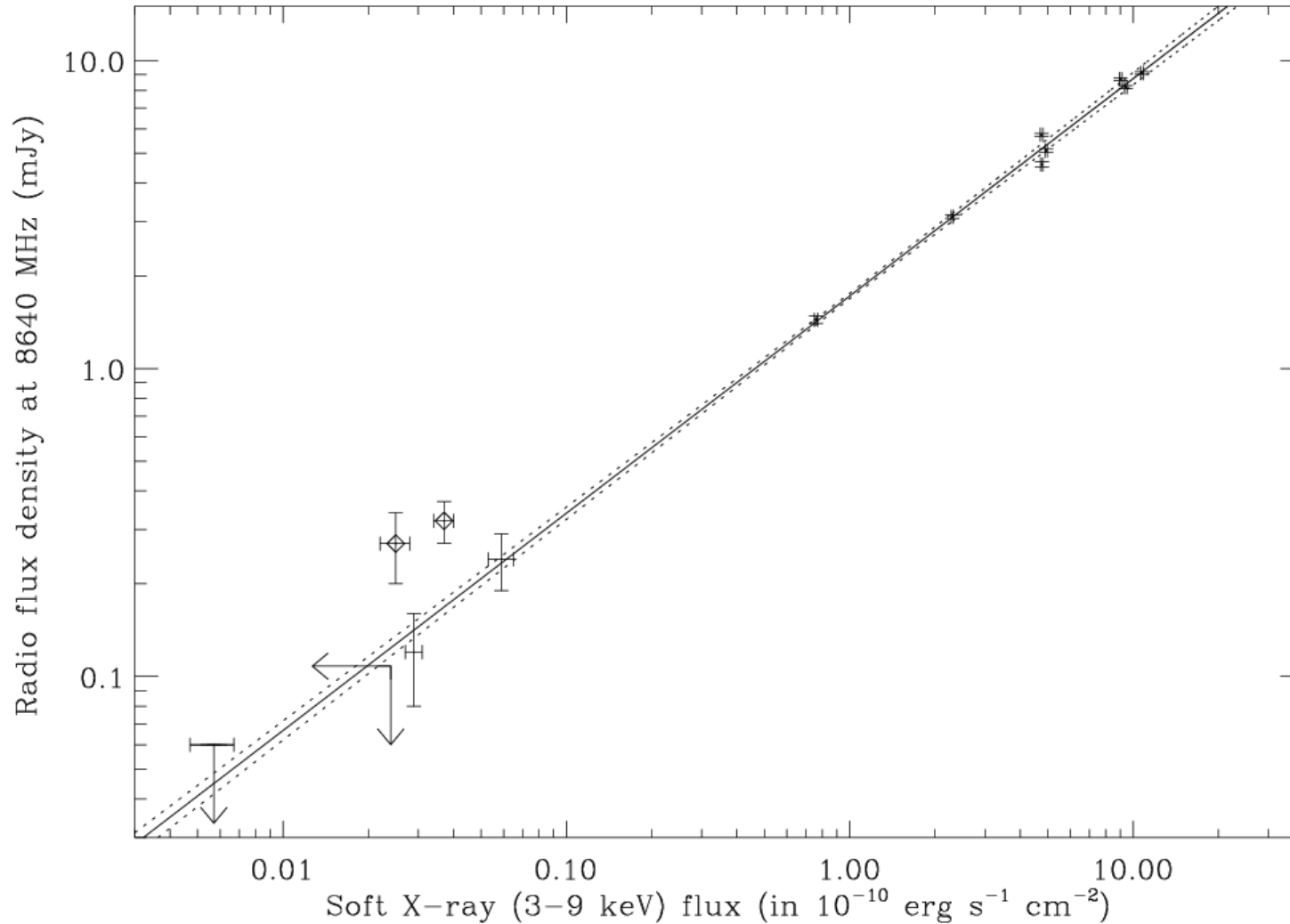
Ron Remillard

Hard

SPL

Thermal

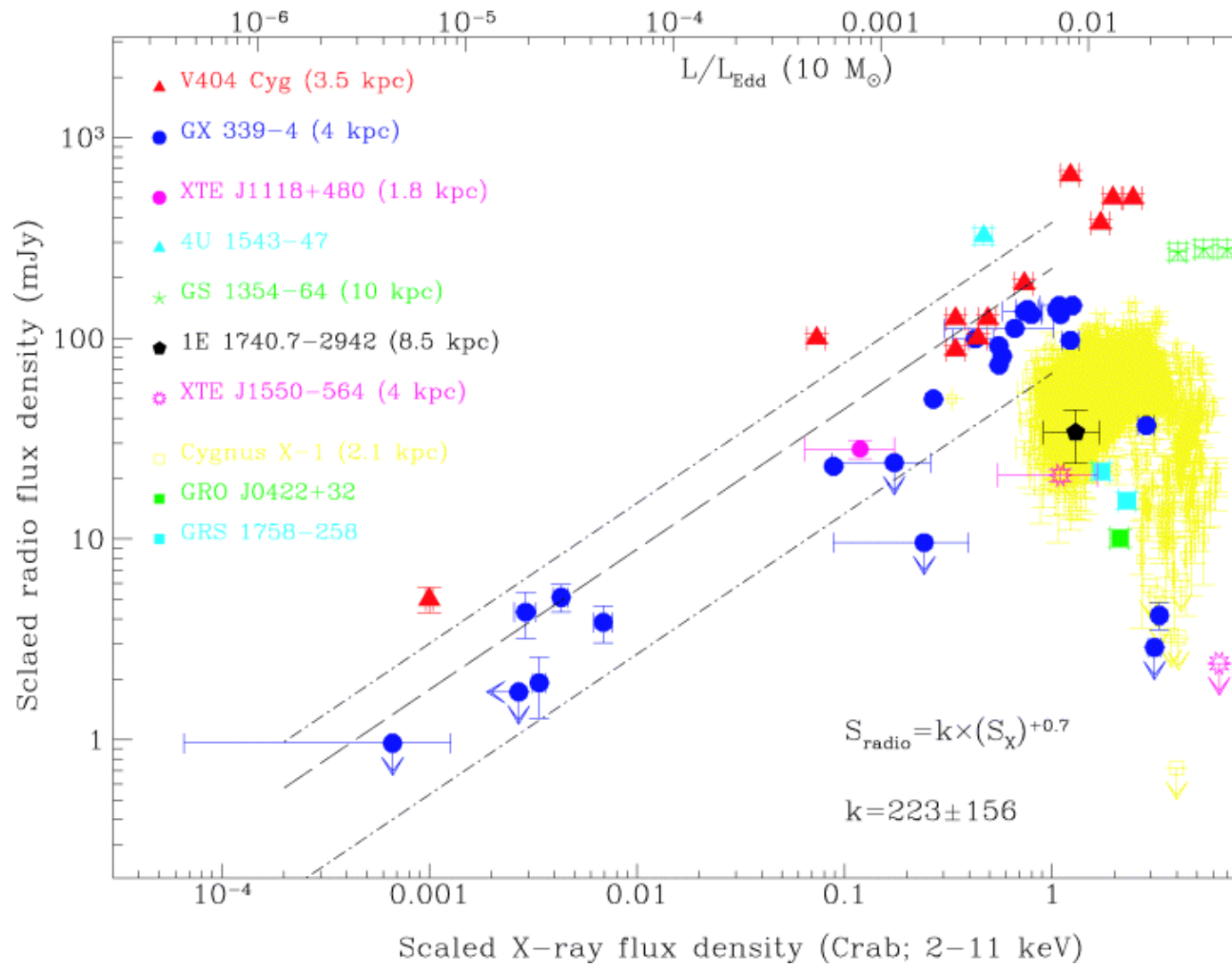
Radio/X-ray Flux Correlation



$$F_{\text{radio}} \propto F_X^{+0.7}$$

Corbel et al. (2000,2003)

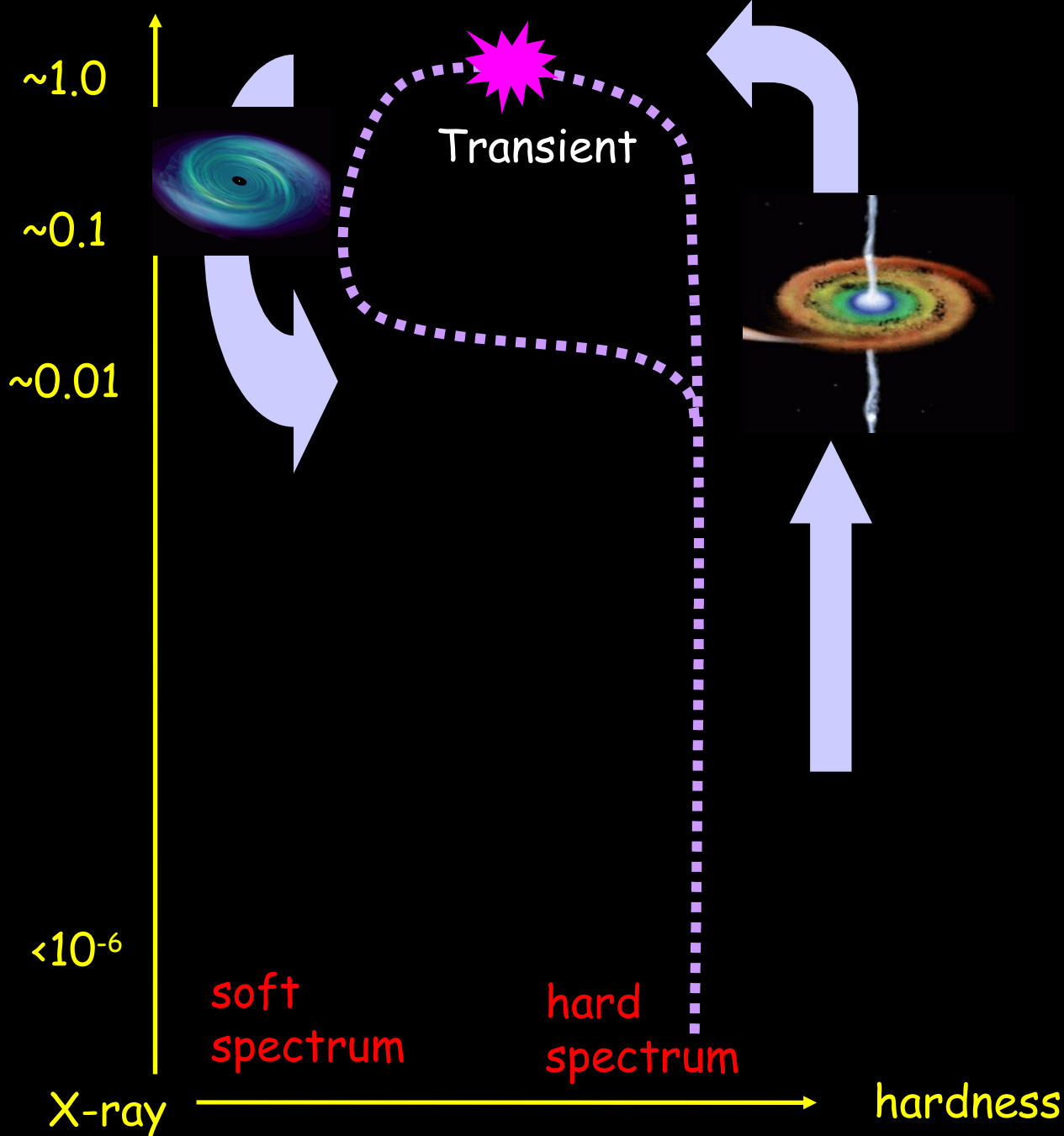
Radio/X-ray Flux Correlation



$$F_{\text{radio}} \propto F_X^{+0.7}$$

Corbel et al. (2000,2003)

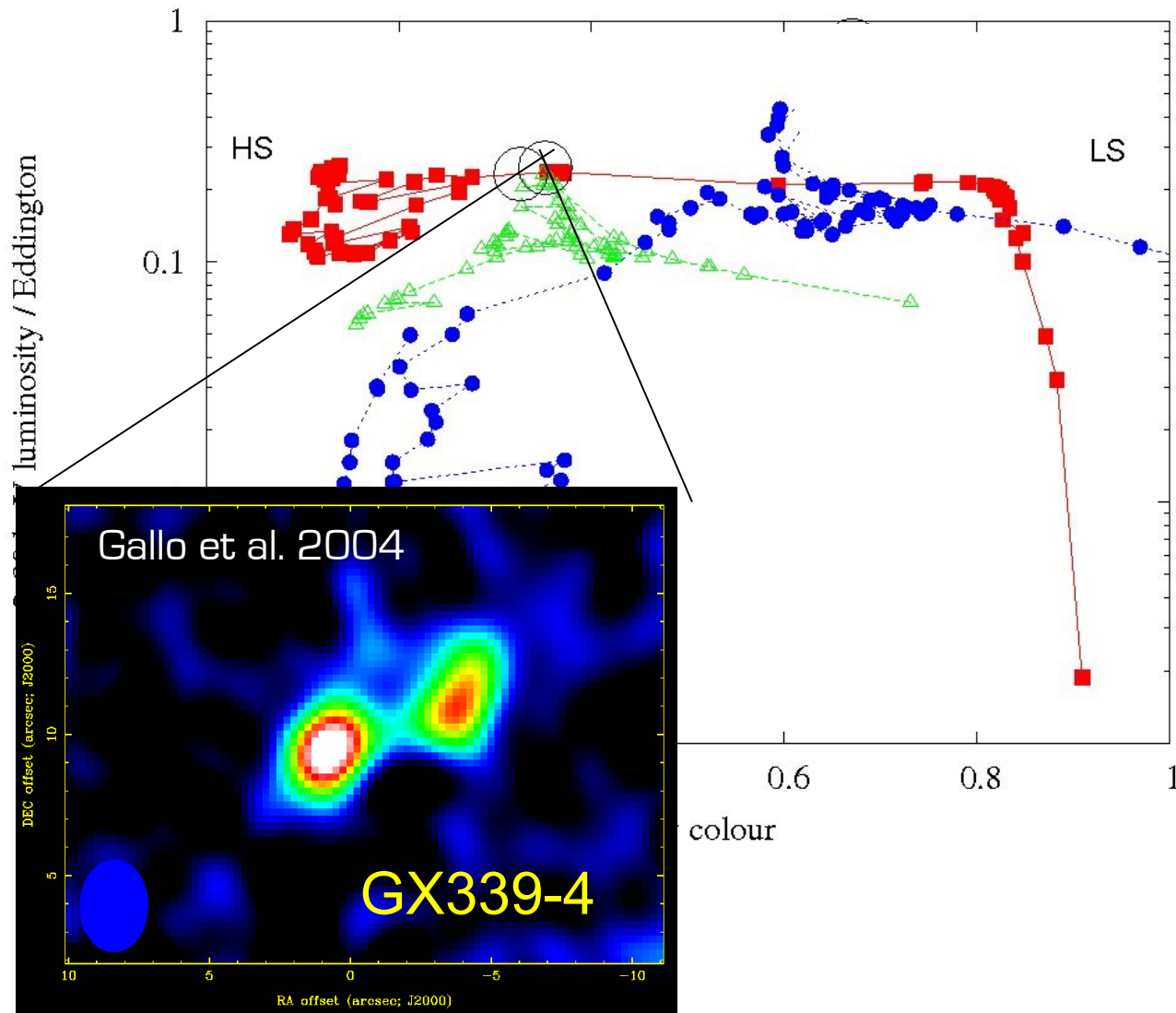
X-ray Luminosity / Eddington



Hardness ratio: the ratio of detector counts in two energy bands

(example. the ratio of source counts at 6.3–10.5 keV to the counts at 3.8–7.3 keV)

Powerful jets
produced in
transition from
canonical
'low/hard' to
'high/soft' states...



Fender, Belloni &
Gallo (2004)

Gallo et al. 2004

Homan & Belloni
2005

<http://www.astro.lsa.umich.edu/Events/Meetings/mctpwww/contrib.html>
Fender.ppt

Black Hole States: Statistics

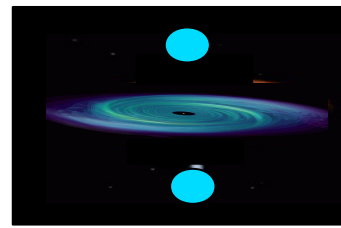
Timescales (days) for state (all BH Binaries)

	<u>duration</u>	<u>transitions</u>
Steep Power Law	1-10	<1
Low/hard	3-200	1-5

Ronald Remillard

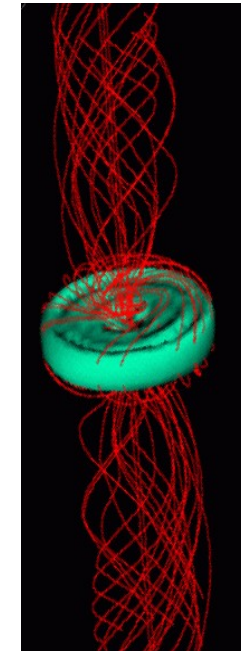
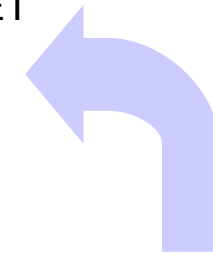
In analogy with solar flares, magnetic energy is probably built-up and accumulated over long time scales and then dissipated in very short time

On the other hand the removal of angular momentum via the steady jet has a dramatic effect on the overall process of the accretion process, further increasing the twist of the magnetic field and making **magnetic reconnection** among tangled field lines likely to occur.



TRANSIENT

JET

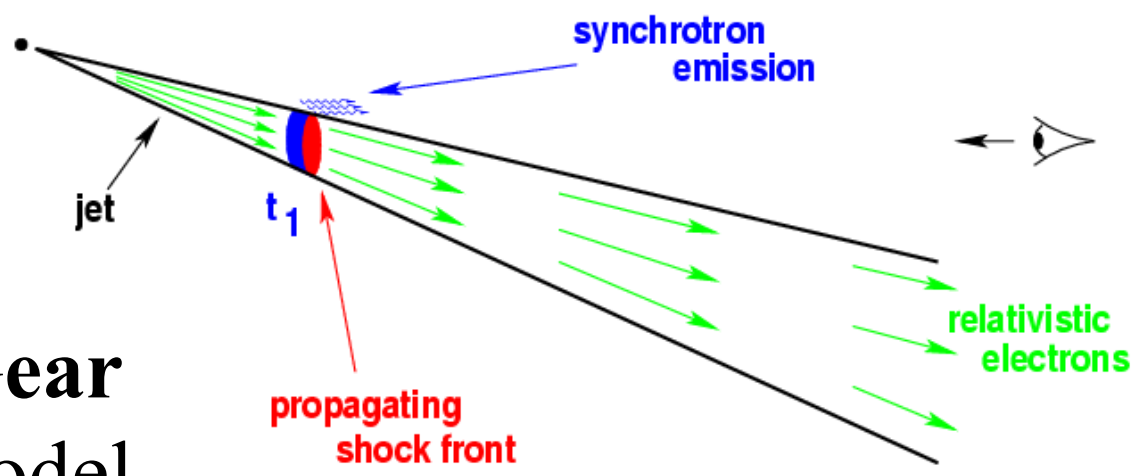


S
T
E
A
D
Y

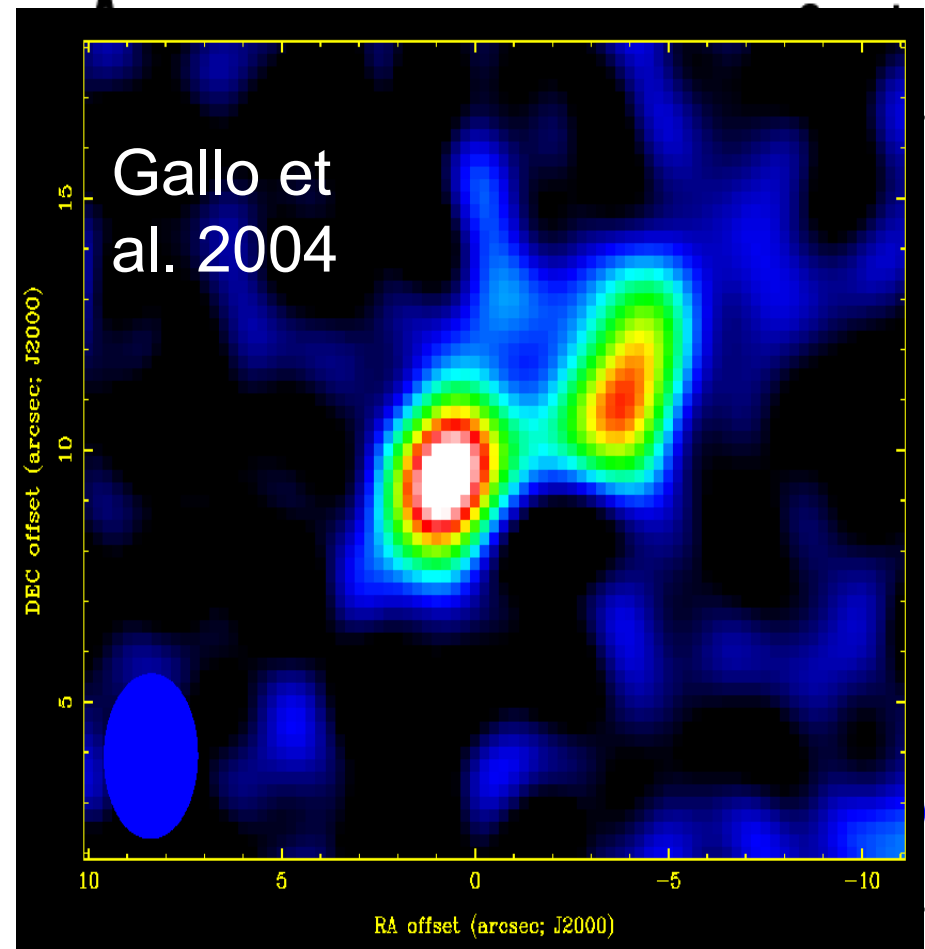
J
E
T

Marscher & Gear shock-in-jet model (1985)

New highly-relativistic
plasma catches up the
pre-existing
slower-moving material
of the **steady jet**
giving rise to shocks...



<http://isdc.unige.ch/~turler/jets/>



Marc
Türler's
review

..that produce
the optically
thin outburst.